DANMARKS OG GRØNLANDS GEOLOGISKE UNDERSØGELSE RAPPORT 2005/19

Preliminary analysis of ultrasonic and geochemical properties of core samples from Glyvursnes-1 and Vestmanna-1, Faroe Islands

Contribution to the SeiFaBa project
Funded by the Sindri group

GEUS

DANMARKS OG GRØNLANDS GEOLOGISKE UNDERSØGELSE RAPPORT 2005/19

Preliminary analysis of ultrasonic and geochemical properties of core samples from Glyvursnes-1 and Vestmanna-1, Faroe Islands

Contribution to the SeiFaBa project
Funded by the Sindri group

Peter Japsen & Regin Waagstein

Released 01.01.2008

GEOLOGICAL SURVEY OF DENMARK AND GREENLAND
MINISTRY OF THE ENVIRONMENT

GEUS

Contents

1. Introduction

A study of the physical properties, petrography and chemical composition of selected core samples from the Faroe Islands has been conducted as part of the SeiFaBa project. The aim of the project is to improve our understanding of the seismic properties of basalt successions.

The continuous core from the new Glyvursnes-1 well (see Waagstein & Andersen 2003) has been density scanned in eighty short intervals with lengths between 12 and 80 cm. Based on this scanning, sixty short sections of constant or almost constant density were selected for petrographical and chemical analysis and a subset for analysis of physical properties. Supplementary measurements of physical properties were carried out on a small number of core samples from the old Vestmanna-1 well. These were taken immediately above or below core intervals for which rock chemical data had been published (Waagstein & Hald 1984).

Plugs with a diameter of 1.5 inch and a length of 3-4 cm were drilled vertically for the rock physical measurements. All plugs were analysed for porosity, permeability and grain density. A subset was also analysed ultrasonically (Olsen 2005). Nineteen samples from Glyvursnes-1 were investigated under both dry conditions and water saturated conditions. Twelve samples from Vestmanna-1 were investigated under water saturated conditions, and two of them also under dry conditions. All sonic samples were measured at hydrostatic conditions at 100, 200 and 300 bar, except three samples where the condition of the sample required the measuring programme to be reduced. Two samples fell apart during the experiment so data are not available at 300 bar. Two samples were also measured at 500 bar in both dry and water saturated condition. The programme comprised measurement of both P- and S-wave velocities.

2. Relation between sonic properties, porosity and lithology

In this chapter we study the acoustic properties of the 28 water saturated core samples at the highest confining pressure available for all samples, 300 bar (Table 2.1). We choose to use the second of the measurements made at that pressure; i.e. the measurement made after the samples had been left to equilibrate in the core holder for a night.

In figures 2.1 to 2.4 plots of Vp and Vs versus porosity for samples of basalt (lava core, lava crust and breccia) and sediments are shown. The data reveal a general trend of increasing velocity, both P and S, as porosity is reduced (Figs 2.1, 2.2). Porosity ranges from 0.7 % to c. 31.8 %, Vp range from 2.8 to 6.6 km/s and Vs from 1.4 to 3.7 km/s. In the plot of Vp versus Vs we observe a very consistent relation with only one data point deviating significantly from the general trend (sample V-10) (see also Olsen 2005). Vp-Vs ratios are typical around 1.8 to 1.85, but two sediment samples have Vp/Vs around 2 and one core sample has a very deviating value, also at 2 (Figure 2.4). This first inspection indicates that the data are of good quality and only one data point appears to be questionable.

The data set can be divided into three group according to lithology: Lava core with porosities below c. 10 %, lava crust and breccia with porosities between c. 10 % and 20 % and sediments with porosities between 24 % and 32 % (3 samples) (Figs 2.1 – 2.4). The relation between velocity and porosity for these three lithologies follow the same trend, but two high-porosity sediment samples have significantly higher Vp-Vs ratio than the lava samples. Moreover, samples of lava crust have slightly higher Vp-Vs ratio than samples of lava core (Fig 2.4).

Comparison with a modified upper Hashin-Shtrikman bound

In a previous report the mineral point for the Lopra-1 well was estimated from the upper limits of Vp, Vs and density based on log data (Mavko et al. 2004; Japsen et al. in press). The values of the bulk modulus, K, and the shear modulus, G, were found to be:

K=91 GPa, G= 43 GPa, rho=3.07 g/cm^3

In Figures 2.1 to 2.7 we compare the data with a modified upper Hashin-Shtrikman bound (MUHS) (see Mavko & Japsen 2005). The *unmodified*, upper bound describes the acoustic properties of the stiffest possible rock as porosity varies between 100 % and 0 % where the properties of the rock is defined by the mineral end point. We can visualise a rock falling on or near the upper bound as being extremely strong and rigid, with extremely stiff pores that are nearly all spherical in shape. A *modified* upper Hashin-Strikman bound describes the properties of the water-saturated rock as porosity varies between 0 % and the *critical porosity*. The critical porosity for basalts refers to the total porosity at the point when the rock would fall apart. It has been shown that the MUHS provides an excellent description of the trend extending from the mineral to the critical porosity. While it is not rigorously a bound, it tends to describe the stiffest rocks in the dataset.

We can obtain a first-order fit with the core data and a modified upper Hashin-Strikman bound by assuming a critical porosity of 30 % and changing the mineral point slightly (compared to that given above):

K=85 GPa, G= 42 GPa, rho=3.07 g/cm^3 (A)

In figs 2.2 and 2.3 we see that the match between the core data and the model is reasonable. A third estimation of the mineral point for the Lopra data was made by Mavko & Japsen (2005) based on analysis of sonic data compared to the neutron porosity log. Because the neutron porosity overestimates porosity (c. 10 % at low porosities) the mineral properties were overestimated due to the projection to 0 % (K=120 GPa; G=50 GPa; rho= 3.31 g/cm^3).

The mineral point value for K given by (A) is in agreement with the maximum value of the bulk modulus estimated for the samples of 85 GPa, and similarly the mineral point value for G matches the maximum value for the core data of 41 GPa. There is also good agreement between the estimates of maximum Vp for basalt based on the ultrasonic data and on the logging data for the Lopra-1 well: Maximum Vp for the logging data is between 6.5 and 7 km/s and maximum for the core data is 6.6 km/s. Maximum Vs for the logging data is between 3.6 and 3.8 km/s and maximum for the core data is 3.7 km/s.

The model is based on a fairly small critical porosity of only 30 % to match the data. The critical porosity is the limit where the rock falls apart and consequently the limit of the shear modulus is 0 GPa at that value. This means that the Poisson ratio is 0.5 and the Vp-Vs ratio approaches infinity because Vs is 0 km/s. The data material is too limited to verify if this is a reasonable assumption because of the few data points with high porosity (Figure 2.4). We see, however, that two sediment samples with high porosities have higher Vp-Vs ratio than the most of the samples. It is not possible to distinguish if this is a property of the sediments because of their high clay content or if these samples represent high-porosity basalt and thus has a high Vp-Vs ratio as predicted by the Hashin-Strikman bound reflecting the properties of the grain contacts in the matrix.

Figures 2.5 to 2.7 show the same data where the data points are distinguished by well rather than by lithology. The data material is too limited to show if there is any systematic difference between the wells, but it appears that the low-porosity Glyvursnes-1 data are slightly stiffer than the data from Vestmanna-1 (closer to the MUHS bound). The Vs measurement for sample V-10 is clearly outlying (Figure 2.3; see also Olsen 2005).

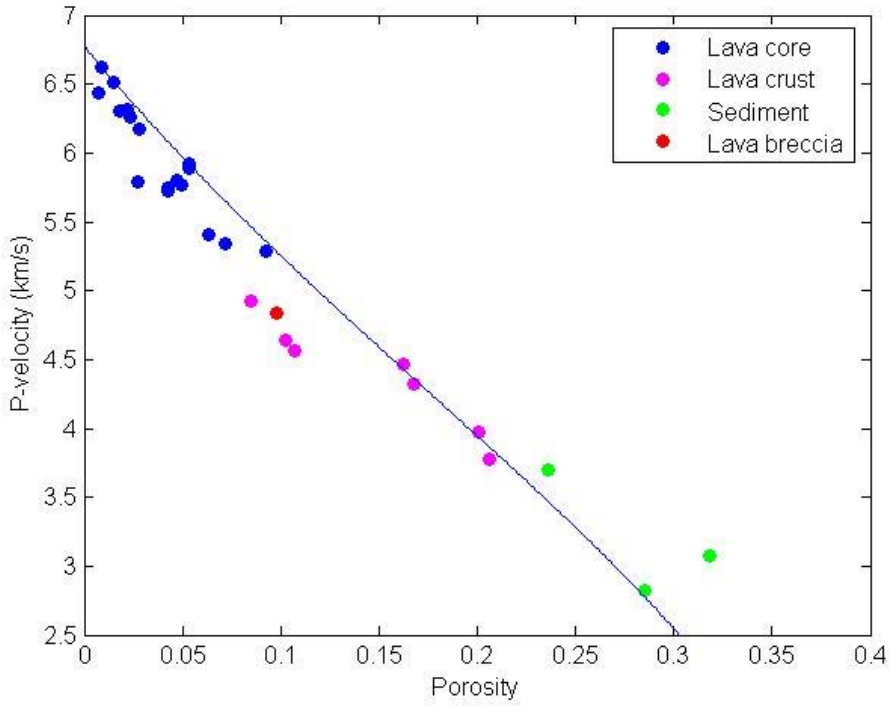

Figure 2.1. *Plot of Vp versus porosity for ultrasonic data from water saturated core samples from the Glyvursnes-1 and Vestmanna-1 wells measured at 300 bar (colour coded by lithology). Modified upper Hashin-Strikman bound shown for reference.*

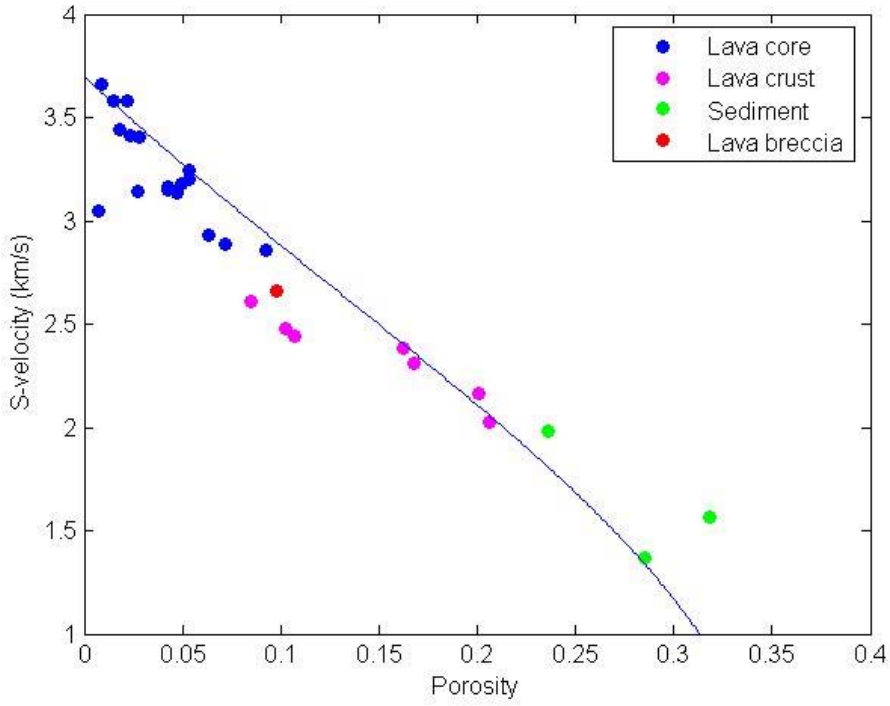

Figure 2.2. *Plot of Vs versus porosity for ultrasonic data from water saturated core samples from the Glyvursnes-1 and Vestmanna-1 wells measured at 300 bar (colour coded by lithology). Modified upper Hashin-Strikman bound shown for reference.*

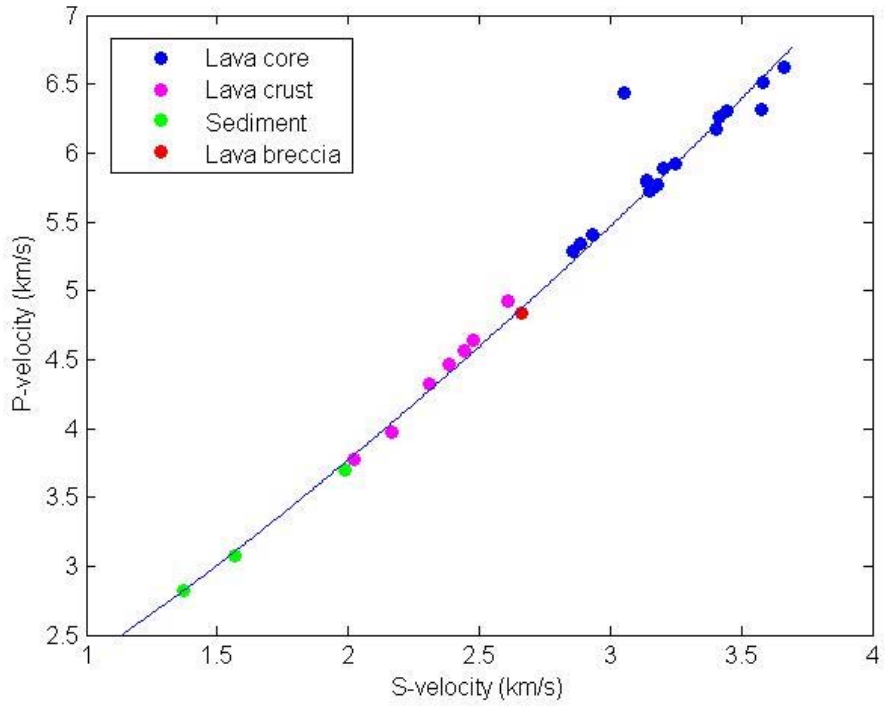

Figure 2.3. *Plot of Vp versus Vs for ultrasonic data from water saturated core samples from the Glyvursnes-1 and Vestmanna-1 wells measured at 300 bar (colour coded by lithology). Modified upper Hashin-Strikman bound shown for reference.*

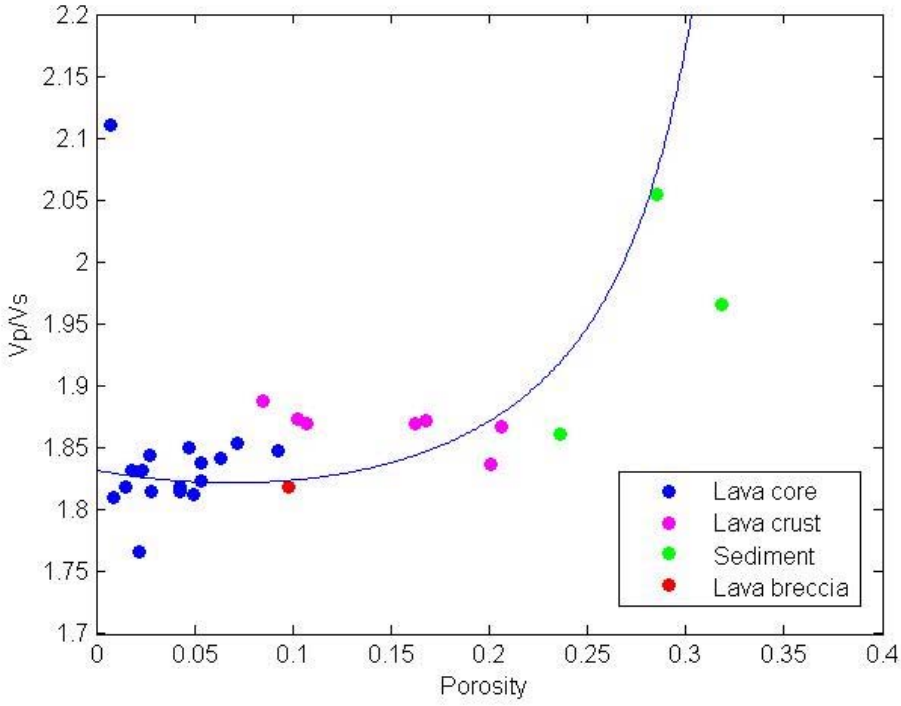

Figure 2.4. *Plot of Vp-Vs ratio versus porosity for ultrasonic data from water saturated core samples from the Glyvursnes-1 and Vestmanna-1 wells measured at 300 bar (colour coded by lithology). Modified upper Hashin-Strikman bound shown for reference.*

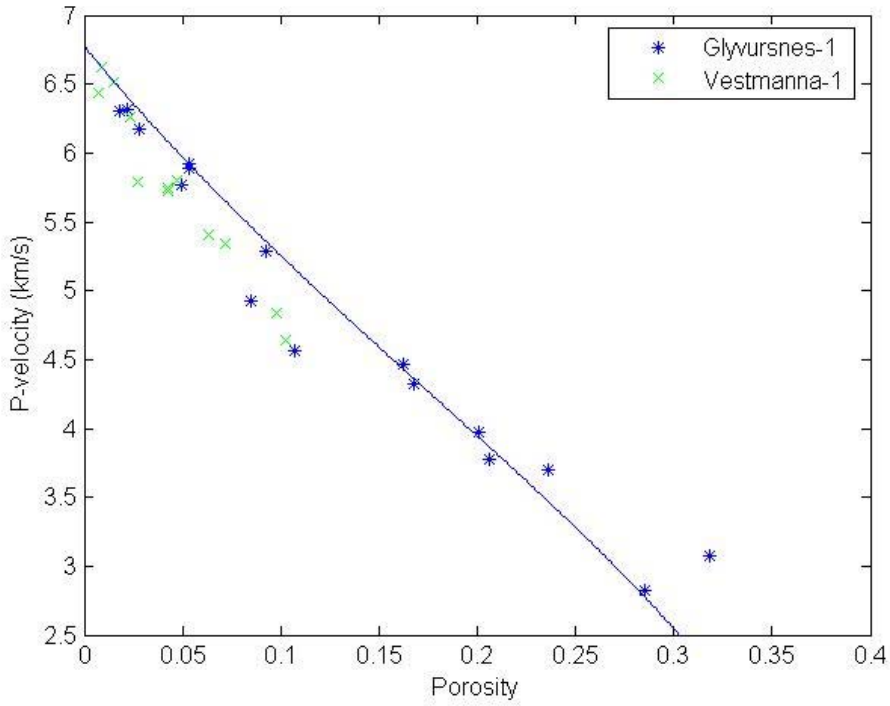

Figure 2.5. *Plot of Vp versus porosity for ultrasonic data from water saturated core samples from the Glyvursnes-1 and Vestmanna-1 wells measured at 300 bar (colour coded by well). Modified upper Hashin-Strikman bound shown for reference.*

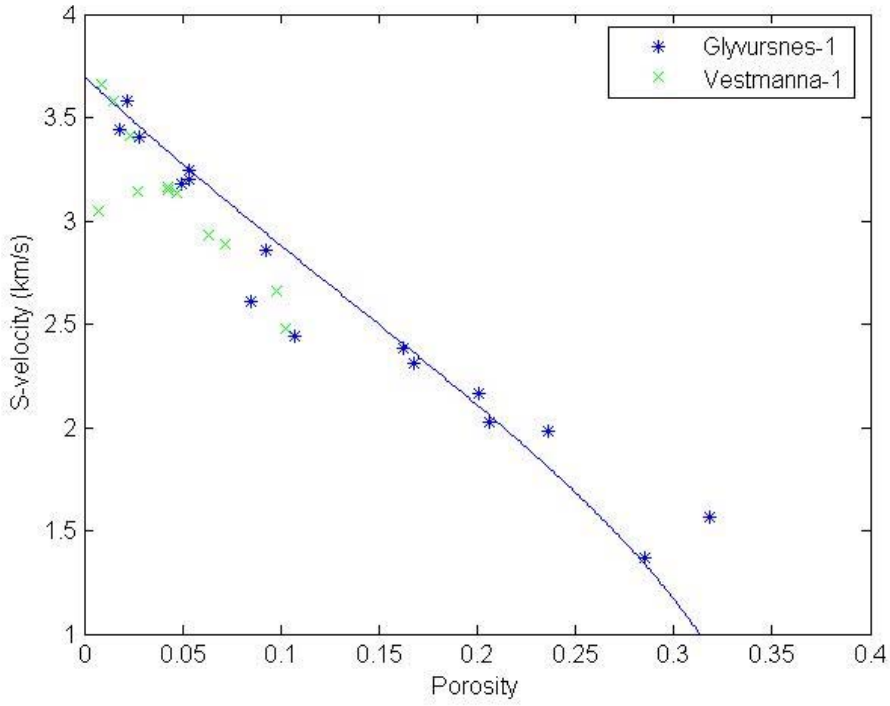

Figure 2.6. *Plot of Vs versus porosity for ultrasonic data from water saturated core samples from the Glyvursnes-1 and Vestmanna-1 wells measured at 300 bar (colour coded by well). Modified upper Hashin-Strikman bound shown for reference.*

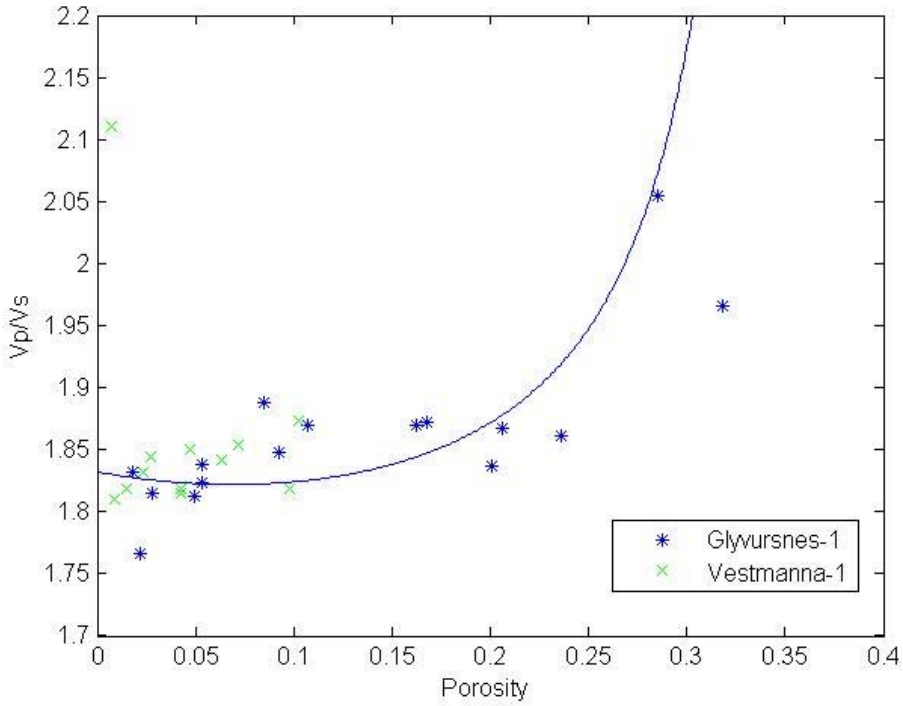

Figure 2.7. *Plot of Vp-Vs ratio versus porosity for ultrasonic data from water saturated core samples from the Glyvursnes-1 and Vestmanna-1 wells measured at 300 bar (colour coded by well). Modified upper Hashin-Strikman bound shown for reference.*

Table 2.1. *Properties of the investigated samples at 300 bar confining pressure (after Olsen 2005).*

Core samples									
ID	**Top depth**	**phi**	**Vp**	**Vs**	**Lith**	**Rho -sat.**	**Rho -dry**	**permea-bility**	**grain density**
	(m)	(%)	(m/s)	(m/s)		(g/cm^3)	(g/cm^3)	(Darcy)	(g/cm^3)
G-06	36.05	4.9	5770	3182	1	2.94	2.91	0.00	3.05
G-07	38.89	31.8	3079	1567	3	2.21	1.89	0.06	2.78
G-12	70.78	10.7	4565	2442	2	2.77	2.68	0.30	2.99
G-13	102.72	2.8	6176	3402	1	2.96	2.94	0.01	3.02
G-19	217.82	20.6	3776	2022	2	2.55	2.35	0.11	2.95
G-20	224.85	16.8	4327	2312	2	2.73	2.57	0.58	3.09
G-32	306.58	16.2	4461	2386	2	2.70	2.56	0.31	3.05
G-35	346.54	8.5	4925	2609	2	2.59	2.53	0.05	2.70
G-36	353.20	2.2	6320	3578	1	2.83	2.82	0.01	2.86
G-37	355.13	23.6	3695	1985	3	2.42	2.20	6.81	2.84
G-40	381.76	5.3	5887	3203	1	2.86	2.83	0.03	2.96
G-50	470.87	9.2	5281	2858	1	2.89	2.81	0.01	3.09
G-71	606.17	28.5	2819	1372	3	2.31	2.02	1.20	2.83
G-75	627.27	20.1	3974	2164	2	2.64	2.44	0.21	3.04
G-76	662.82	5.3	5919	3246	1	2.87	2.84	0.01	2.98
G-77	668.62	1.8	6305	3443	1	2.85	2.84	0.01	2.87
V-02	149.04	9.8	4836	2660	4	2.72	-	0.01	2.90
V-03	157.30	10.3	4642	2478	2	2.73	2.65	1.79	2.93
V-04	165.00	7.2	5346	2884	1	2.83	-	0.01	2.98
V-05	180.92	4.7	5804	3138	1	2.92	-	0.01	3.02
V-06	181.83	4.3	5727	3149	1	2.87	-	0.01	2.95
V-07	201.03	1.5	6509	3580	1	3.06	-	0.00	3.09
V-08	287.09	2.3	6256	3415	1	2.95	-	0.01	3.00
V-10	361.43	0.7	6436	3050	1	2.95	2.94	0.00	2.95
V-12	484.89	0.9	6626	3661	1	3.07	-	0.00	3.08
V-13	500.36	4.3	5742	3163	1	2.90	-	0.02	2.97
V-14	514.20	6.3	5403	2934	1	2.86	-	0.02	2.98
V-17	582.90	2.7	5790	3140	1	2.92	-	0.00	2.96

ID: G Glyvursnes-1, V Vestmanna-1.

lith: 1 lava core, 2 lava crust, 3 sediment, 4 breccia.

3. Comparison between core and log data

The log measurements in the Glyvursnes-1 and the Vestmanna-1 wells have been estimated at the same depths as where the core samples were taken: e.g. density, neutron porosity, Vp and Vs. The log readings are compared with the lab data in Figs 3.1 to 3.4.

Table 3.1. *Log measurements at the depth of the investigated samples (see Table 2.1.).*

Well log										
ID	**GR**	**Resistivit**	**NPHI**	**Density**	**Vp**	**Vs**	**Vp_bc**	**Vs_bc**	**Vp_geus**	**Vs_geus**
	(API)	(ohm·m)	(%)	(g/cm^3)	(m/s)	(m/s)	(m/s)	(m/s)	(m/s)	(m/s)
G-06	15.5	2240	8.2	2.85	5738	2977	6060	3213	5470	3076
G-07	38.5	635	38.5	2.36	3050	1686	3109	1702	4881	2444
G-12	7.0	730	17.2	2.75	4437	2488	4495	2454	4395	2427
G-13	12.4	5704	5.9	2.86	5857	3405	5867	3397	6183	3307
G-19	12.3	512	25.8	2.59	3361	1935	3384	1962	3359	1798
G-20	7.9	781	19.5	2.73	3285	1708	3393	1842	3553	1856
G-32	4.9	652	19.3	2.73	4076	2189	4011	2151	4184	2410
G-35	10.7	1921	35.4	2.61	4421	2477	4431	2434	4700	2443
G-36	5.9	23421	12.2	2.83	6390	3629	6467	3708	6728	3718
G-37	49.8	560	22.6	2.56	3755	2146	3928	2209	3807	2011
G-40	10.8	3333	11.9	2.76	5917	3372	5784	3377	5543	3196
G-50	8.2	2095	12.1	2.81	4802	2749	4809	2756	4887	2709
G-71	59.8	401	44.7	2.34	2288	1305	2141	1216	2978	1739
G-75	10.7	1018	26.1	2.68	4100	2308	4137	2317	4126	2105
G-76	14.4	3789	11.9	2.80	5439	3076	5433	3078	5458	3080
G-77	6.4	15601	15.2	2.83	6024	3480	6079	3495	6615	3452
V-02	5.6	2185	20.1	2.74	4645	2663	4658	2660	4821	2709
V-03	9.7	1577	20.0	2.75	4693	2662	4709	2639	4663	2610
V-04	16.3	3317	11.7	2.80	5107	2833	5106	2834	5081	2846
V-05	9.6	2711	10.0	2.83	5411	3123	5456	3092	5470	3126
V-06	4.3	2185	13.4	2.80	5454	3014	5410	3057	5470	2994
V-07	7.8	5409	8.0	2.87	6181	3471	6219	3468	6465	3512
V-08	5.3	5285	8.4	2.83	6004	3379	5951	3380	6321	3346
V-10	6.4	8389	10.0	2.85	6256	3457	6246	3455	6465	3469
V-12	10.3	5718	7.3	2.89	6385	3565	6370	3568	6465	3555
V-13	6.9	1200	15.6	2.81	5357	3083	5388	3050	5321	2995
V-14	10.5	1849	17.1	2.82	5285	2873	5237	2939	5418	2802
V-17	5.3	2801	13.6	2.84	5465	2973	5467	2969	5470	3026

Vp and Vs log readings of Vp and Vs by LogTek ('Guided peak finding routine').

Vp- and Vs-bh: pseudo borehole compensated reading by LogTek.

Vp- and Vs-GEUS: semblance processing by GEUS.

See Waagstein & Andersen (2003) for further details about the processing of the full waveform sonic.

Table 3.2. *Difference between various measurements on 28 water saturated core samples (300 bar) and the corresponding log readings from Glyvursnes-1 and Vestmanna-1.*

Core – log	Unit	Mean	Std.	Min	Max	Figure
Density (saturated) – density	g/ccm	0.035	0.081	-0.151	0.188	3.1
Porosity – NPHI	%	-7.8	5.3	-27	1	3.2
Vp – Vp	m/s	258	245	-126	1042	3.3
Vp – Vp-bh	m/s	238	273	-290	934	(3.3)
Vp – Vp-GEUS	m/s	75	450	-1802	774	(3.3)
Vs – Vs	m/s	36	178	-407	603	3.4
Vs – Vs-bh	m/s	22	169	-405	470	(3.4)
Vs –Vs-GEUS	m/s	9	242	-877	456	(3.4)

Vp and Vs log readings of Vp and Vs by LogTek ('Guided peak finding routine').
Vp- and Vs-bh: pseudo borehole compensated reading by LogTek.
Vp- and Vs-GEUS: semblance processing by GEUS.
See Waagstein & Andersen 2003 for further details about the processing of the full waveform sonic.

Log displays of Vp versus depth are shown in Figs. 3.5 to 3.8 (Glyvursnes-1) and 3.9 to 3.12 (Vestmanna-1). The ultrasonic data for the core samples are also displayed in these plots.

The comparison of core and log density shows a good correlation, but for high core densities (c. 3 g/ccm) all core plugs have significantly higher densities than the log readings (Figure 3.1). This may be due to the high-frequent sampling for the core data, but the comparison of core and log Vp-data does not show a similar difference for low porosities.

The comparison of core porosity and the neutron porosity log shows that the neutron porosity overestimates porosity significantly for both high- and low-porosity basalt (mean difference -8 %) (Figure 3.2). There is a tendency that the exaggeration of the neutron porosity is larger for Vestmanna-1 than for Glyvursnes-1 at low porosities.

The comparison of core and log Vp shows a very good correlation (Figure 3.3). Core Vp is slightly higher than the log reading (258 m/s). Maybe due to the finer sampling of spikes in the core material than for the log measurement. The mean difference and standard deviation between the measurements are small for all three interpretations of the sonic log measurement (the semblance processing has the highest standard deviation).

The comparison of core and log Vs also shows a very good correlation (Figure 3.4). Mean difference is only 36 m/s. The estimation of Vs from the full waveform sonic was very complicated (see Waagstein & Andersen 2003), but these results show that the estimate of Vs is just as good as the estimate of Vp.

There is no difference in the correlation between the core and log data between Glyvursnes-1 and Vestmanna-1.

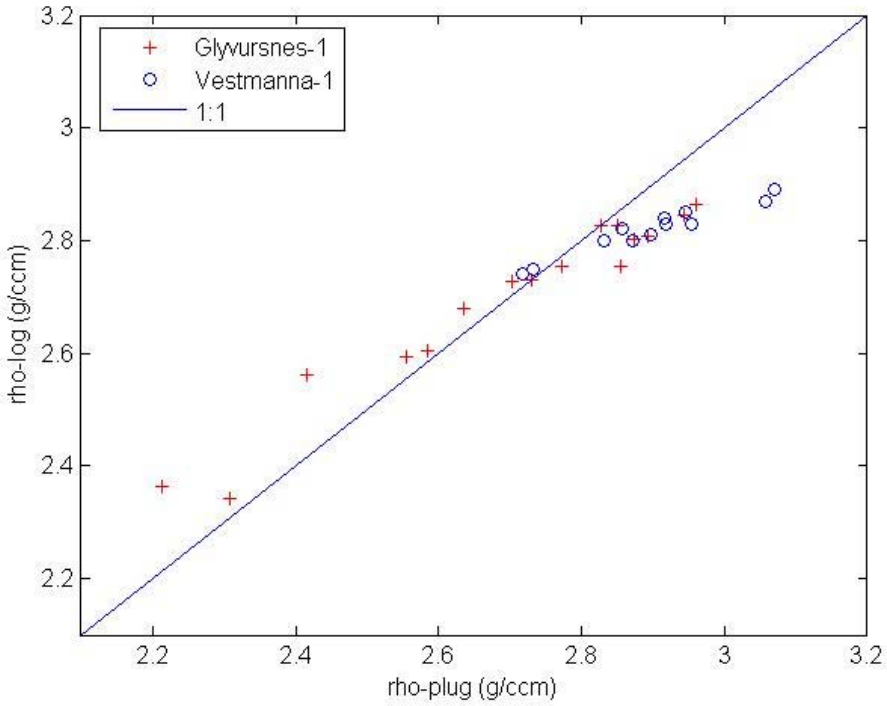

Figure 3.1. *Plot of density estimates (log versus water saturated core data at 300 bar).*

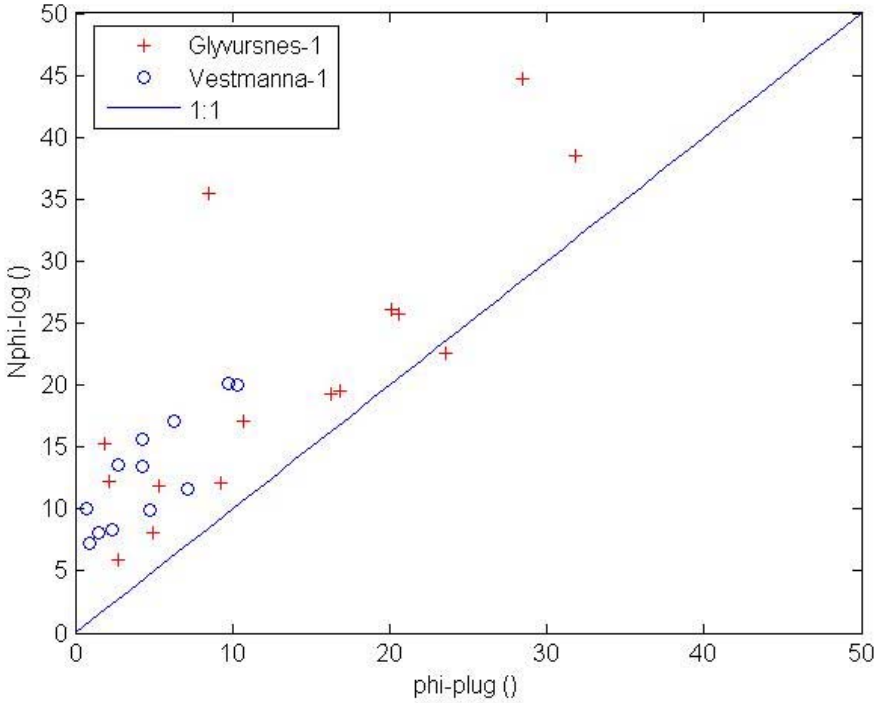

Figure 3.2. *Plot of porosity estimates (neutron porosity log versus water saturated core data at 300 bar).*

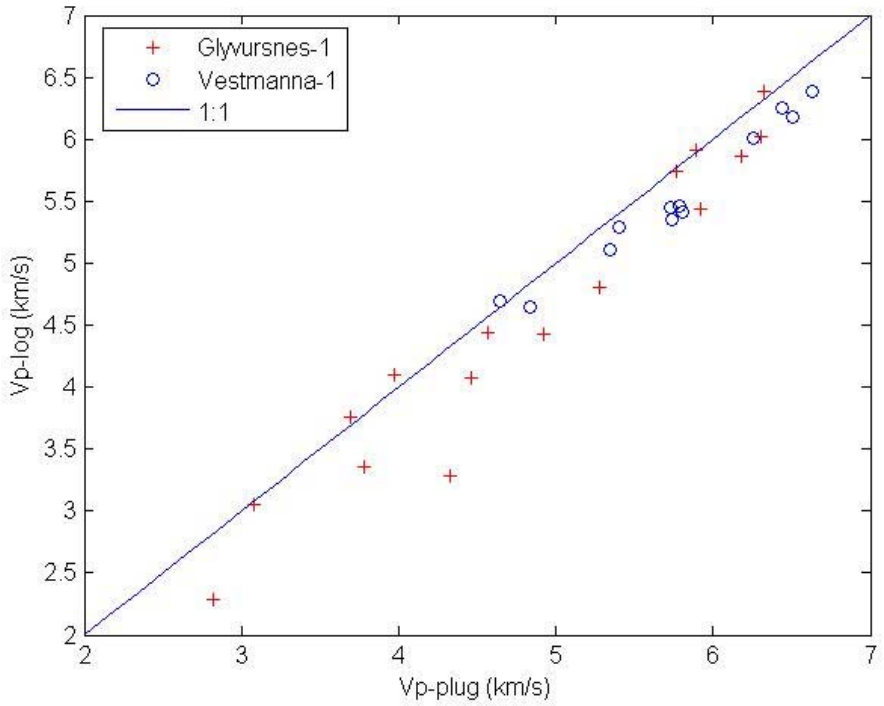

Figure 3.3. *Plot of Vp estimates (log versus water saturated core data at 300 bar).*

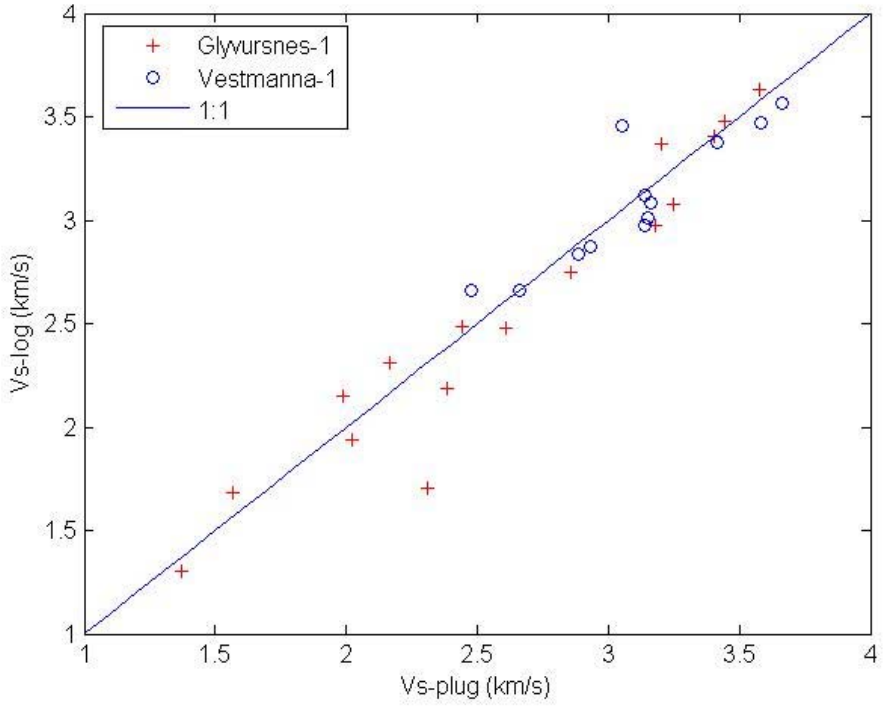

Figure 3.4. *Plot of Vs estimates (log versus water saturated core data at 300 bar).*

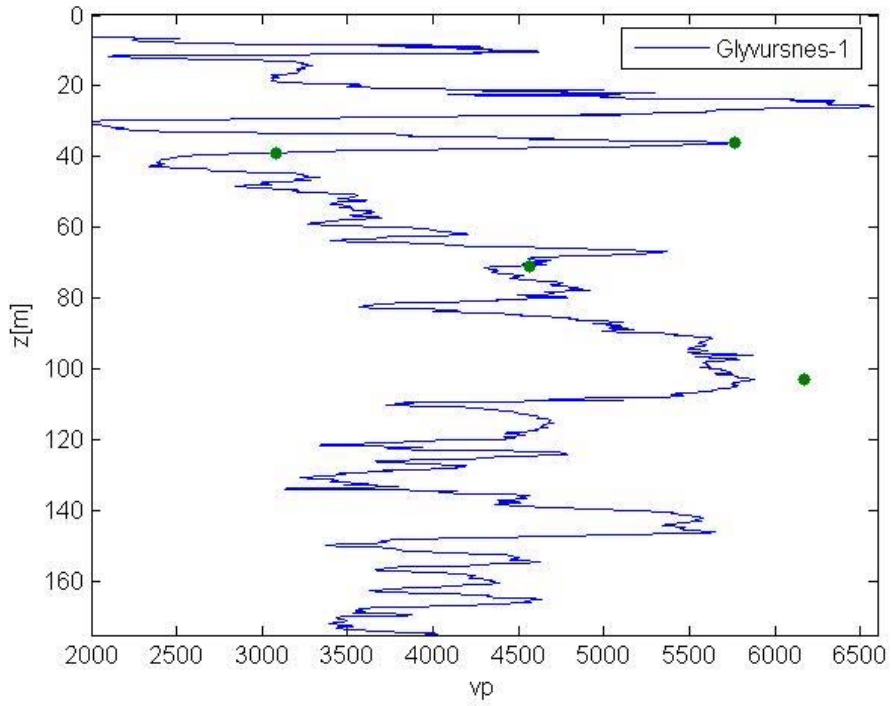

Figure 3.5. *Log plot of Vp versus depth for the Glyvursnes-1 well (0 – 180 m). Core data indicated by dots.*

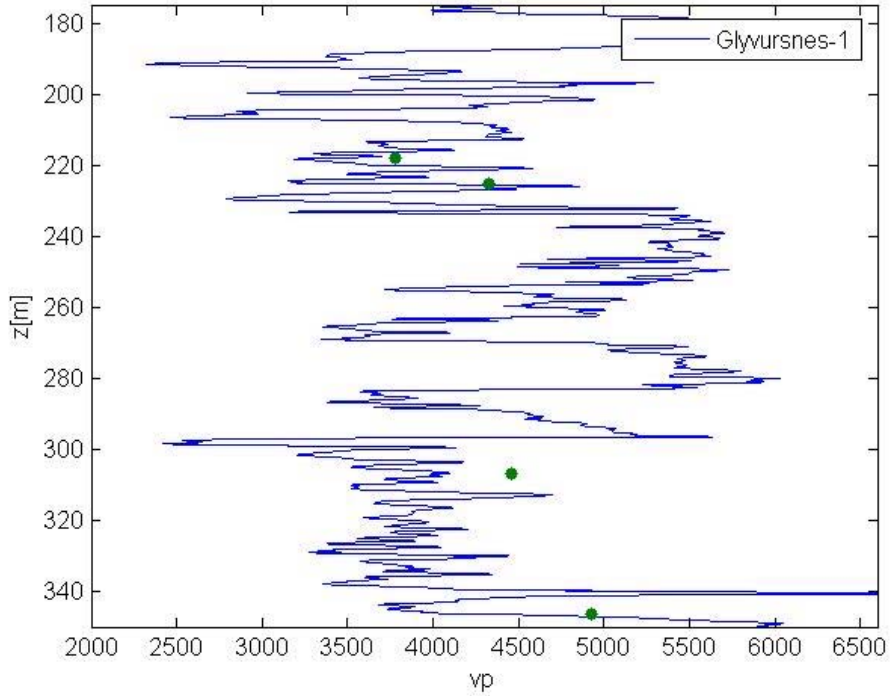

Figure 3.6. *Log plot of Vp versus depth for the Glyvursnes-1 well (180 – 350 m). Core data indicated by dots.*

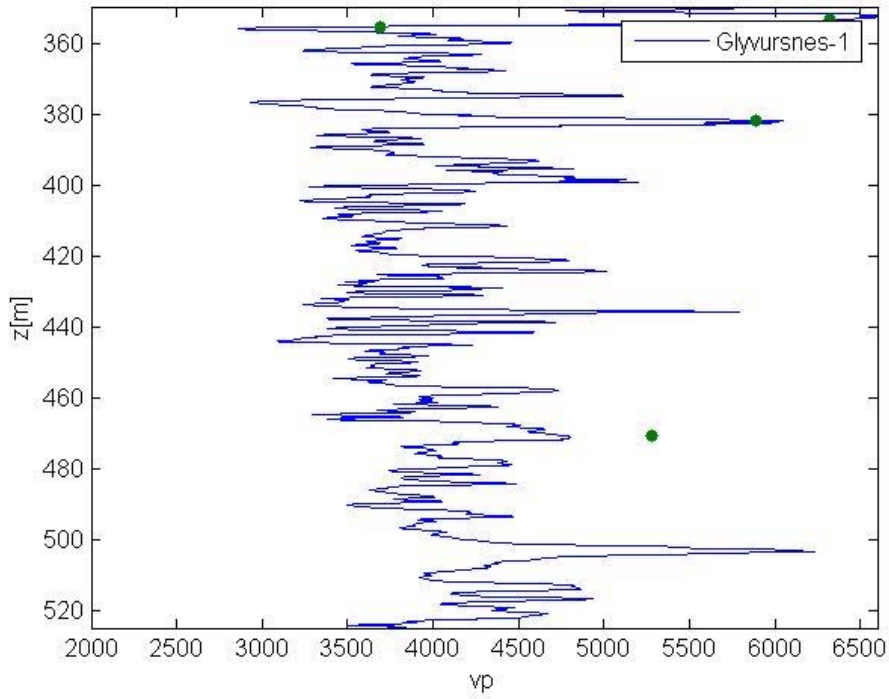

Figure 3.7. *Log plot of Vp versus depth for the Glyvursnes-1 well (350 – 520 m). Core data indicated by dots.*

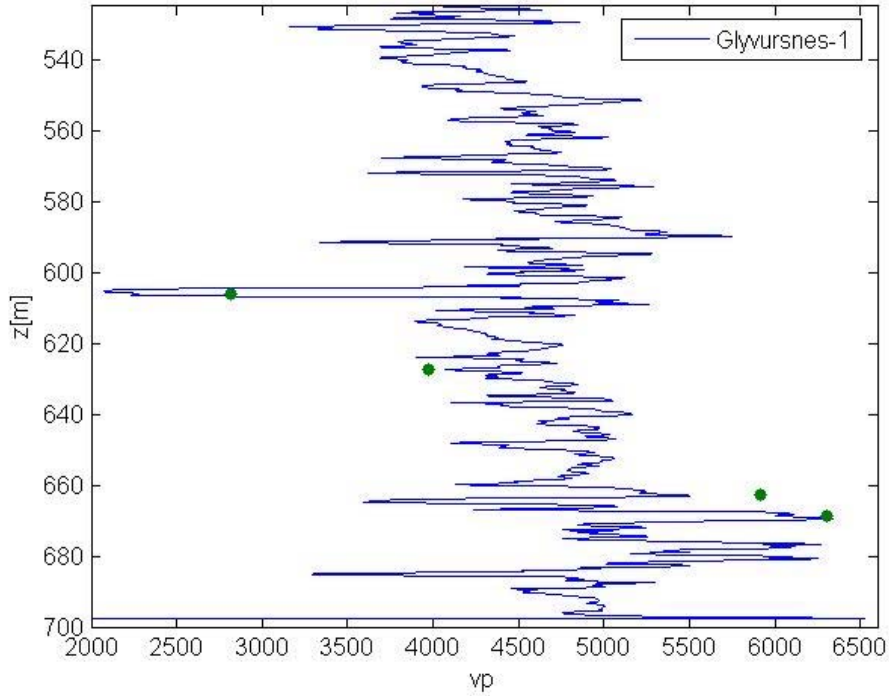

Figure 3.8. *Log plot of Vp versus depth for the Glyvursnes-1 well (520 – 700 m). Core data indicated by dots.*

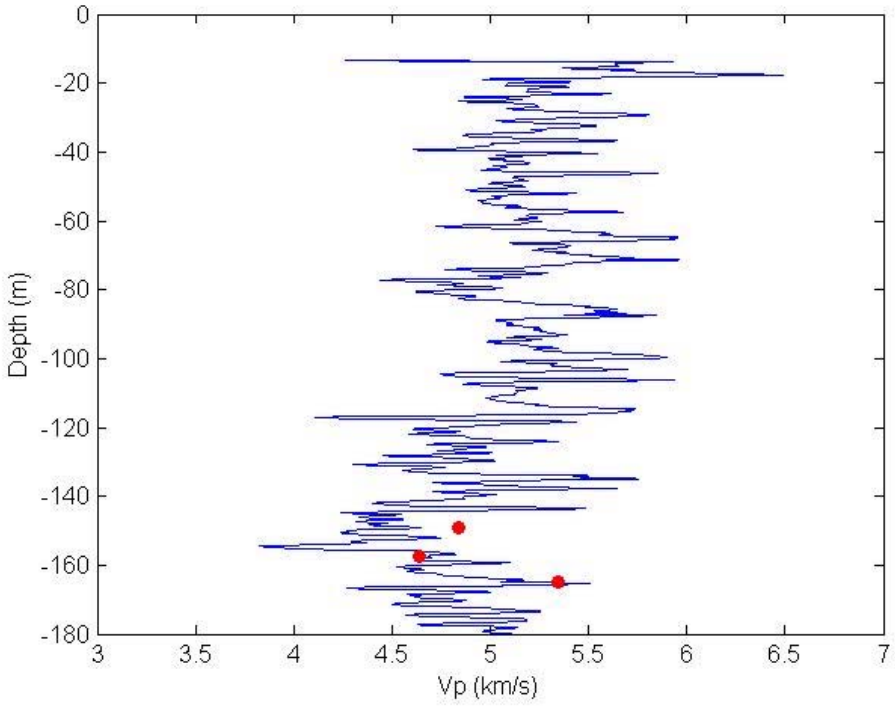

Figure 3.9. *Log plot of Vp versus depth for the Vestmanna-1 well (0 – 180 m). Core data indicated by dots.*

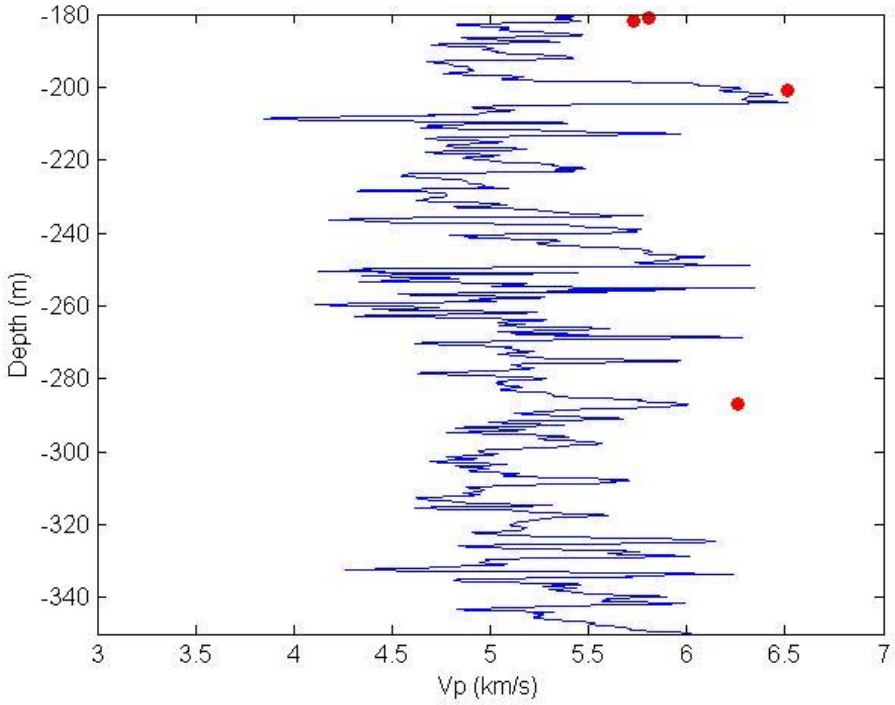

Figure 3.10. *Log plot of Vp versus depth for the Vestmanna-1 well (180 – 350 m). Core data indicated by dots.*

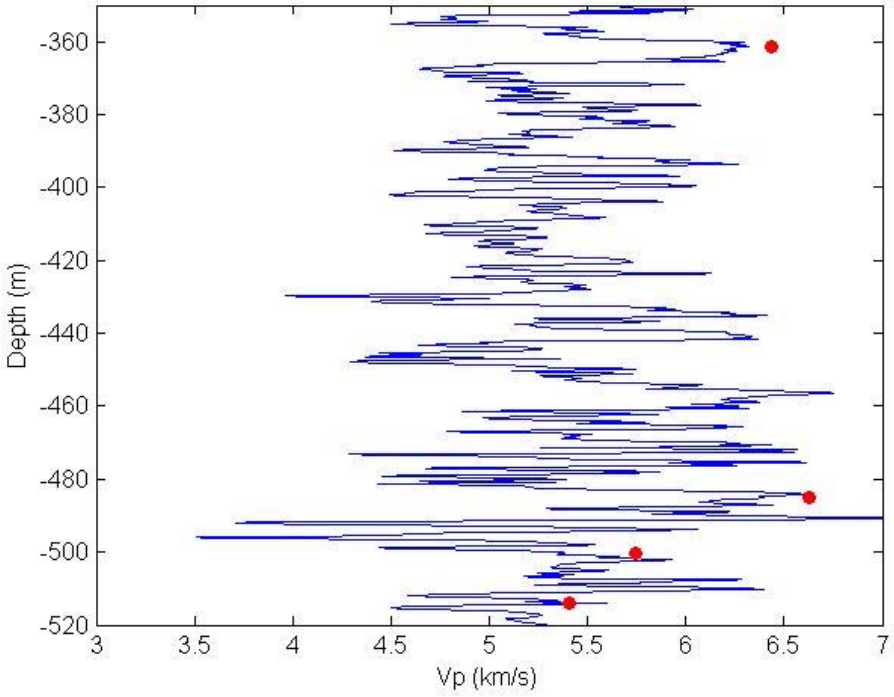

Figure 3.11. *Log plot of Vp versus depth for the Vestmanna-1 well (350 – 520 m). Core data indicated by dots.*

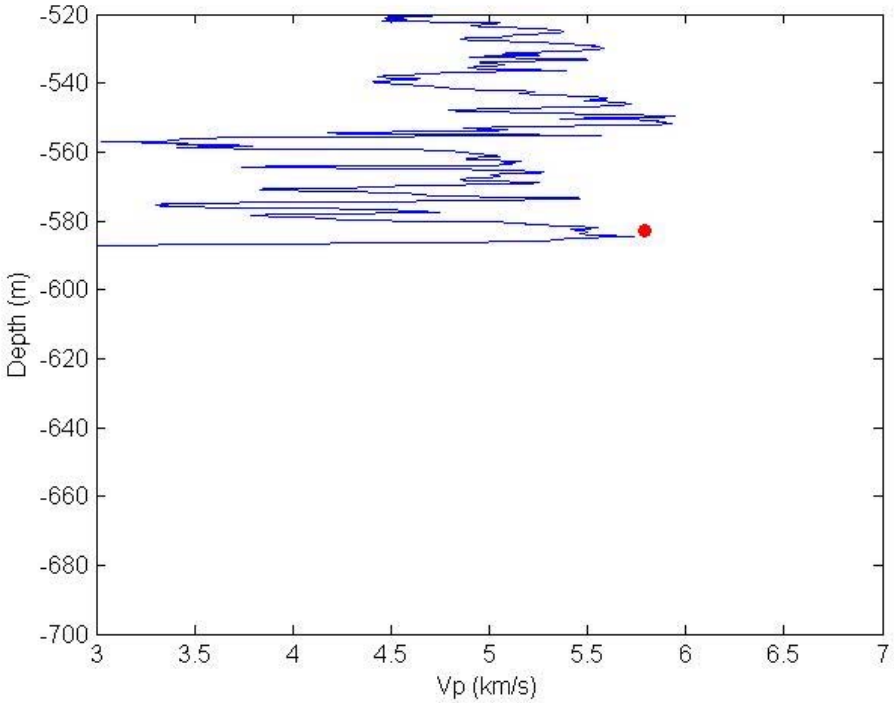

Figure 3.12. *Log plot of Vp versus depth for the Vestmanna-1 well (520 – 580 m). Core data indicated by dots.*

4. Petrography and chemical composition of the Glyvursnes-1 core and correlations with physical properties

Petrography and chemistry

Sixty core samples from the Glyvursnes-1 well have been chemically analysed and examined in thin section. The whole-rock chemical analyses are shown in Appendix A together with the results on some international reference samples. In addition to the major elements, Appendix A also provides some selected trace elements and the CIPW mineral norm computed from the major elements. The petrography is summarised in Appendix B.

The sediments are all tuffs, that is altered volcanic ash. The ash particles are translucent to opaque and consist of completely altered glass with or without microlites. The tuffs contain phenocrysts or fragments of plagioclase usually making up less than 1 % of the rock.

Most basalts are glomerophyric. The glomerocrystic aggregates consist mainly of phenocrysts of plagioclase. However, they are often intergrown with phenocrysts of olivine and sometimes also with small phenocrysts of pyroxene.

The fine groundmass of the basalts consists mainly of plagioclase and pyroxene, but contains in addition small amounts of Fe-Ti-oxides and usually also some olivine. The groundmass contains variable amounts of mesostasis, which consists of clay, zeolites or other secondary minerals replacing interstitial glass or filling interstitial voids. The former glass is often loaded with tiny quenched crystals of the same minerals as the groundmass. Fresh glass is only found in one sample.

The olivine in the basalts is completely replaced by clay or other secondary minerals in all but two samples. The plagioclase is generally fresh although often showing incipient alteration. The pyroxene is almost always completely unaltered.

The basalts contain variable amounts of gas vesicles or tiny pores. The vesicles or pores are usually partly or completely filled with secondary minerals, mostly clay or zeolites. The gas porosity measurements are generally considerably higher than those estimated from thin sections. This suggests that many pores are thinner than the thickness of the thin section (c. 0.03 mm).

The normative mineral composition computed from the major element analyses shows that all but one basalt contain normative hypersthene and either normative quartz or olivine when the FeO/Fe_2O_3 ratio is adjusted to 0.15, which is a normal ratio for unaltered basalts. The basalts are therefore quartz tholeiites and olivine tholeiites.

The chemical analyses confirm the presence of low-Ti basalt identified at two levels by Waagstein & Andersen (2003) based on macroscopic appearance, but also show the presence of a silicic basalt at about 435 m. The analyses also in general confirm the grouping of flow-units into flow groups presented in the same report, although a few should probably be combined.

Correlation of physical properties with mineralogical and chemical composition of cores

The physical properties of rocks are partly related to physical parameters like porosity and fracturing and partly to the mineral composition of the rock matrix. The mineralogy is reflected by the chemical composition of the rock. The influence of mineralogy on the physical properties of the Glyvursnes core is displayed below based on whole-rock chemistry (see Appendix A) using physical property data from core plugs (Vp and grain density, see Table 2.1) or from different wire-line logs (Waagstein & Andersen 2003). The chemical analyses include 'volatiles' determined as the loss on ignition (LOI) corrected for oxidation of iron. The correction is based on the assumption that the FeO of the sample has been completely oxidised to Fe_2O_3 during ignition. LOI in the diagrams below is the same as 'volatiles' in Appendix A. The core plug Vp data plotted in the diagrams are measured under saturated conditions at 300 bar except for two plugs (G-30 and G-34). These fell apart at 300 or 200 bar, respectively, and data at 200 or 100 bar are used instead (Olsen, 2005).

Figure 4.1 shows grain density versus total iron for lava core, lava crust and tuff. The grain density is positively correlated with iron, which element in fresh basalts is residing mainly in Fe-Ti-oxides, pyroxene and olivine. These minerals have a higher density than plagioclase, the other major mineral component of basalt. Furthermore, the iron content and thereby density increases in pyroxene and olivine with the iron content of the original magma. For the same iron content the grain density is systematically lower in lava crust than in lava core for the same iron content. This suggests that a larger part of the iron is residing in clay in the lava crust than in lava core and is in keeping with the higher degree of alteration of lava crusts. The tuffs are all rich in clay and show the lowest grain densities.

Figure 4.2 shows grain density versus loss on ignition (LOI). The latter parameter is measured routinely during chemical analysis and is an indicator of the amount of clay or zeolites. These minerals contain approximately 10 wt.% water in the crystal structure. The water is released when the sample is heated to about 1000°C. Some weight loss could also be due to the breakdown of carbonates, but carbonates are virtually absent in the Glyvursnes samples examined. The grain density is inversely correlated with loss on ignition for all rock types and approaches a minimum density of 2.7 g/cm^3 at a maximum loss on ignition of 8 Wt.%. The rocks with the highest loss are the most altered ones and consist dominantly of water-bearing secondary minerals. The dominant alteration minerals are smectitic clay and various zeolites.

Figure 4.3 shows neutron porosity from borehole logging minus gas porosity from cores taken at the logged depth. Neutron porosity measures the amount of hydrogen whether present in pore water or bound in crystals. It is on average about 8 % too high as compared to gas porosities (see section 3 and Fig. 3.2). This difference may be taken as a measure of mineral bound water. It is plotted in Fig. 4.3 versus the volume of water bound in secondary minerals

estimated from loss on ignition (assuming no carbonates and a grain density of 2.95 g/cm^3). For most cores and logging depths there is a good correlation between the two types of estimates.

Figure 4.4 shows Vp versus pore volume. Vp is taken from the sonic log. The pore volume is neutron log porosity minus mineral bound hydrogen (estimated from LOI). The sample points include all depths from which chemical analysed core samples exist. The plot is similar to Fig. 2.1, which is based on a smaller number of Vp and porosity data measured directly on plugs from both Glyvursnes-1 and Vestmanna-1. Fig. 4.4 shows that when neutron porosity is corrected for fixed water the correlation between Vp and porosity measured by wire-line logging is very similar to that measured on plugs in the laboratory. In general, the measured porosity is higher than the porosity seen in thin section indicating that part of the pores are thinner than 0.03 mm.

Figure 4.5 shows Vp measured on plugs saturated at 300-bar pressure versus total iron content. The velocity is about 6 km/s for lava core, 4-5 km km/s for lava crust and about 3 km/s for tuff. All three lithologies show a tendency of slightly decreasing velocities with iron content. This has no simple explanation.

Figure 4.6 shows Vp measured by wire-line logging at the depth of the core samples versus total iron content of the cores. The wire-line log sonic velocity shows a larger scatter than the velocity from plugs because they are less precise. Nevertheless, the above slight trend of decreasing velocity with iron content seems still to exist for lava core and crust.

Figure 4.7 shows the Vp-Vs ratio from the sonic log versus loss on ignition of cores. Lava crust and tuff have on average a higher Vp-Vs ratio than Lava core. This may be explained by the higher content of clay (and porosity) in the former rocks. However, there is no clear trend with loss on ignition. Some lava core and crust velocity data are exceptionally high. This is not seen in plug data (not shown), which suggests that some high values obtained from the sonic log are not real.

Figure 4.8 shows a good correlation between K_2O content and natural gamma-ray response. The potassium content increases more rapidly than the gamma-ray intensity. This shows that the relative contribution from Th and U is lower in the high-K than in the low-K rocks and suggests that the potassium in the former rocks has been increased by secondary alteration processes. Potassium is known to be highly mobile during such processes, while Th is considered relatively immobile.

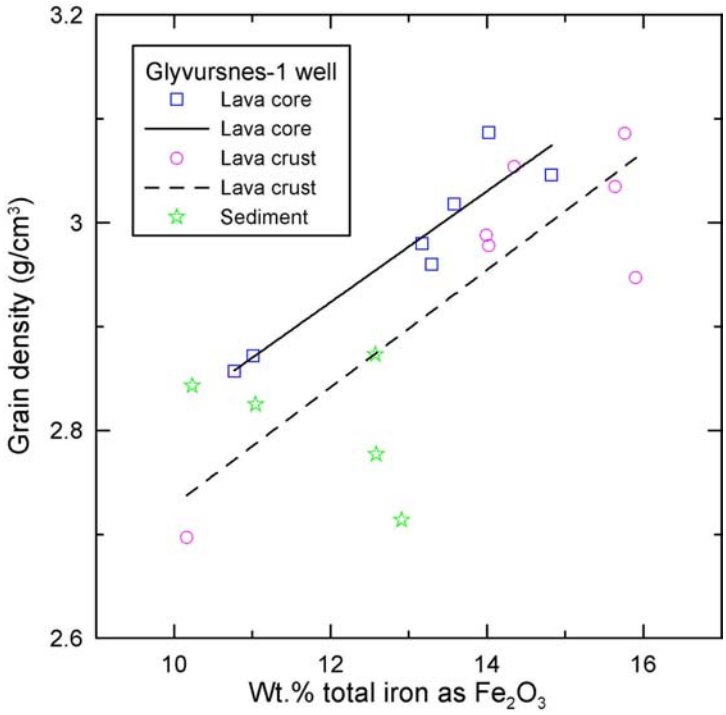

Figure 4.1. *Grain density versus total iron from cores for lava core, lava crust and tuff.*

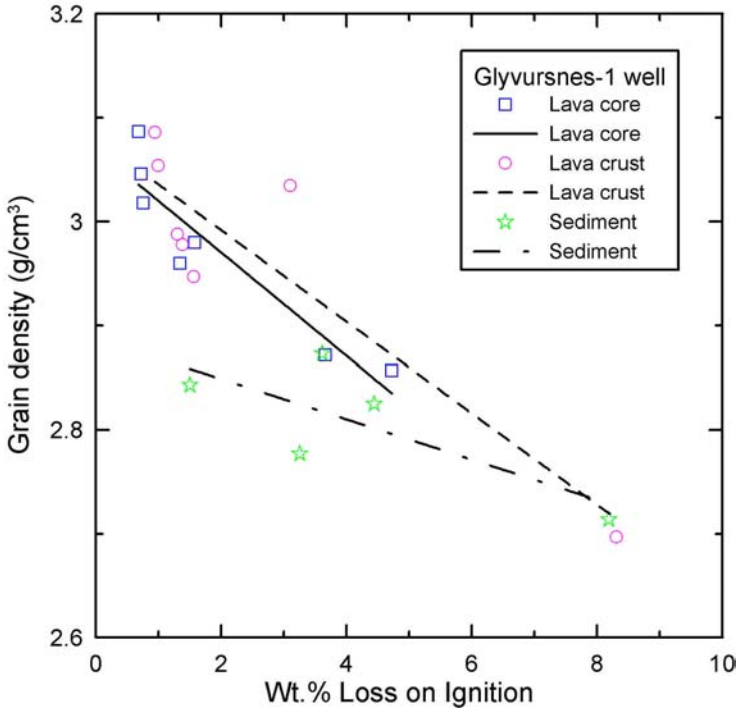

Figure 4.2. *Grain density versus loss on ignition (LOI) from cores.*

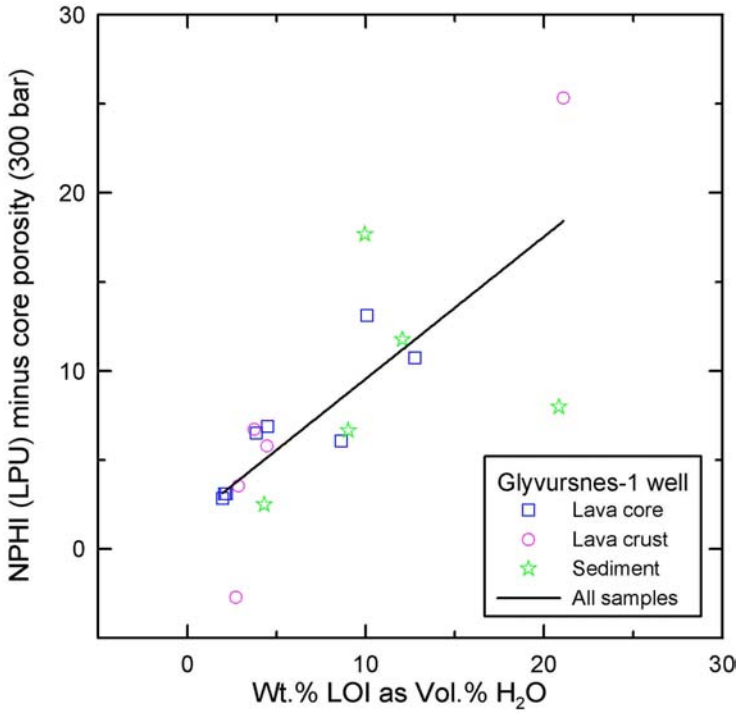

Figure 4.3. *Neutron porosity (log) minus He-porosity (core) versus volume of water bound in secondary minerals. Water volume estimated from loss on ignition (assuming no carbonates and a grain density of 2.95 g/cm3).*

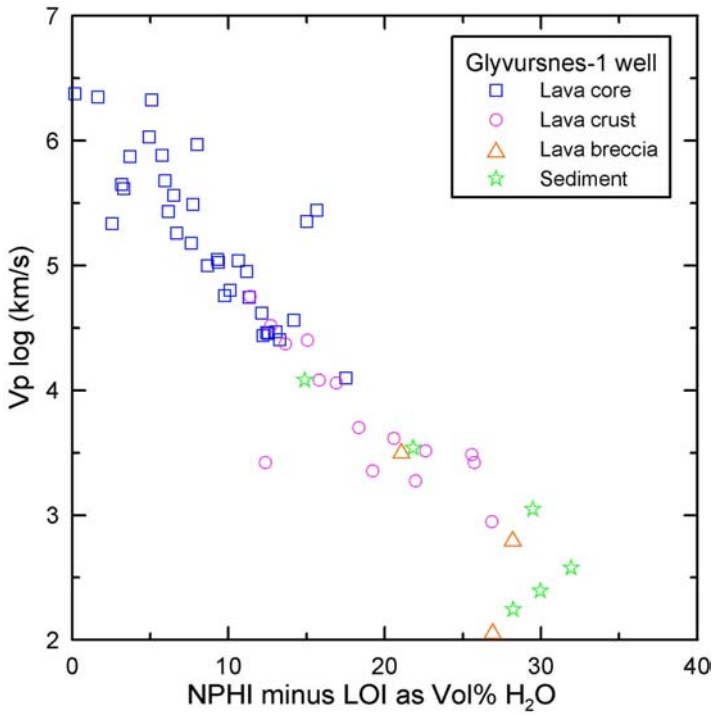

Figure 4.4. *Vp (log) versus pore volume (neutron log porosity minus mineral bound hydrogen estimated from LOI).*

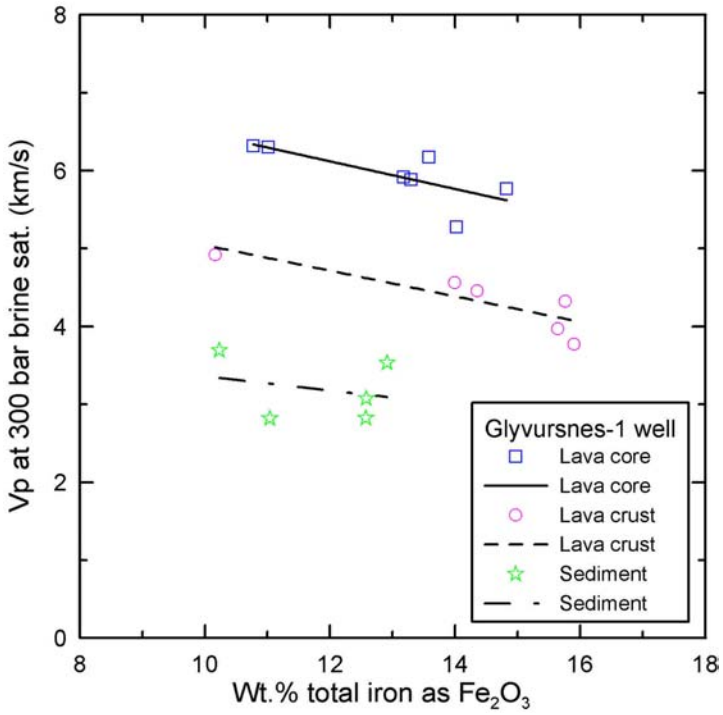

Figure 4.5. *Vp (core) versus total iron content of the cores. Vp measured on water saturated plugs at 300-bar confining pressure.*

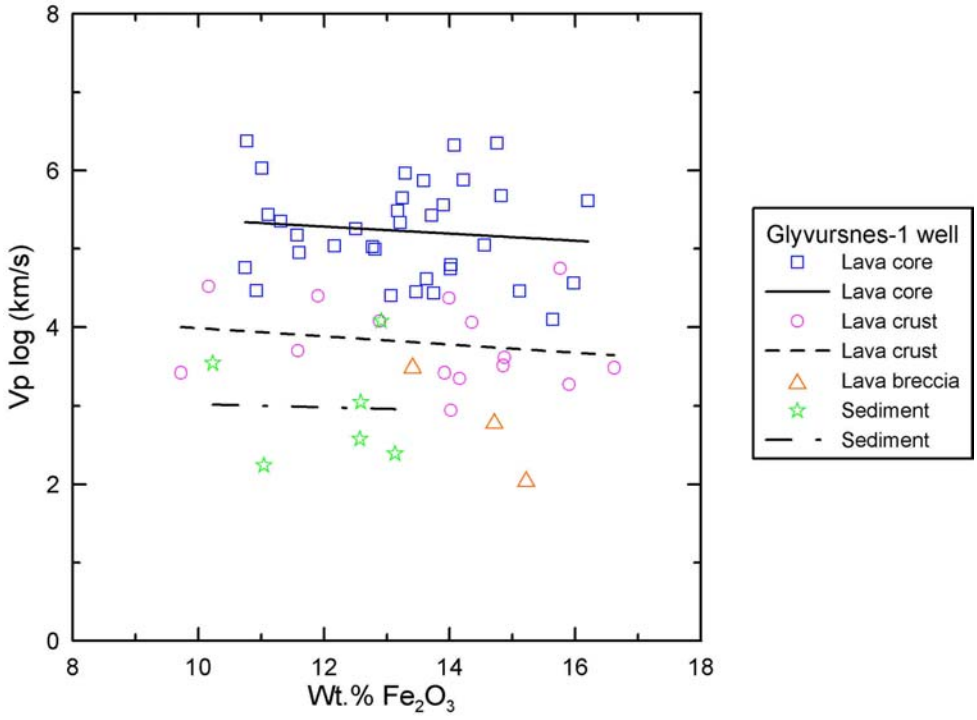

Figure 4.6. *Vp (log) versus total iron content of the cores. Vp measured by wire-line logging at the depth of the core samples*

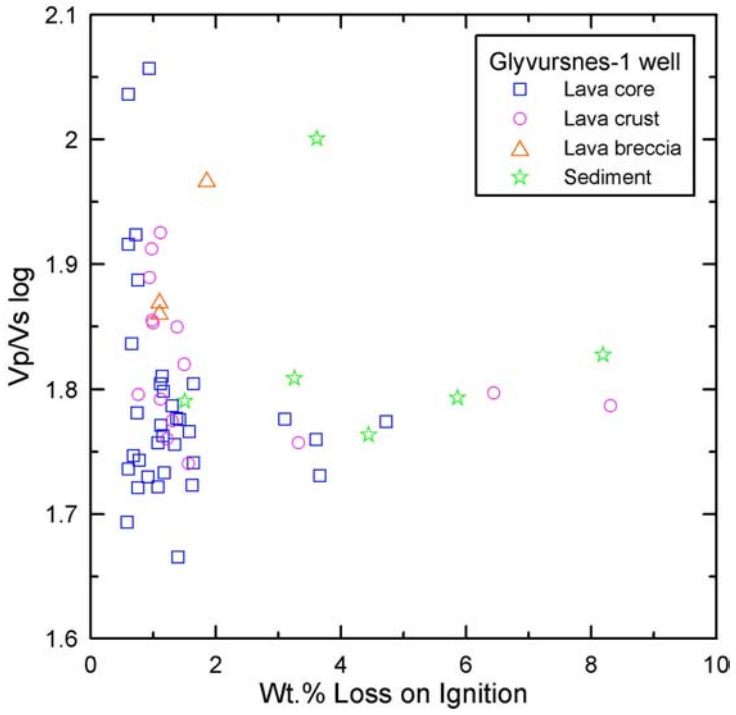

Figure 4.7. *Vp-Vs ratio (log) versus loss on ignition (LOI) of the core samples.*

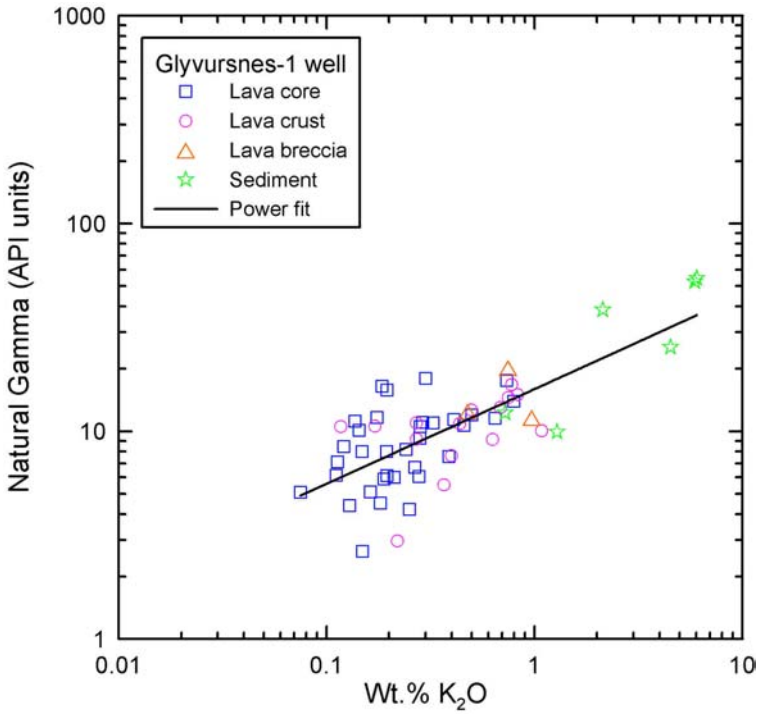

Figure 4.8. *Natural gamma-ray response versus K_2O content of the cores.*

References

Japsen, P., Andersen, C., Andersen, H.L., Boldreel, L.O., Mavko, G., Mohammed, N.G., Pedersen, J.M., Petersen, U.K., Rasmussen, R., Shaw, F., Springer, N., Waagstein, R., White, R.S. & Worthington, M. in press. Preliminary results of petrophysical and seismic properties of Faroes basalts (SeiFaBa project). In: Doré, A.G. & Vining, B. (eds) Petroleum Geology: NW Europe and Global Perspectives: Proceedings of the 6th Conference. Geological Society, London.

Mavko, G., Japsen, P. & Boldreel, L.O. 2004. Preliminary rock physics analysis of basalts in the Lopra-1 well. GEUS rapport 2004/96, 11 pp.

Mavko, G. & Japsen, P. 2005. Rock physics analysis of sonic velocities in wells Lopra-1, Glyvursnes-1 and Vestmanna-1. GEUS Rapport 2005/17, 29 pp.

Olsen, D. 2005. Special Core Analysis for the SeiFaBa Project. Ultrasonic velocity measurements on plug samples from the Vestmanna-1 and Glyvursnes-1 wells, Faroe Islands. GEUS Rapport 2005/10, 65 pp.

Waagstein, R. & Andersen, C. 2003. Well completion report: Glyvursnes-1 and Vestmanna-1, Faroe Islands. GEUS rapport 2003/99, 67 pp.

Waagstein, R. & Hald, N. 1984. Structure and petrography of a 660 m lava sequence from the Vestmanna-1 drill hole, lower and middle basalt series, Faeroe Islands. In: Berthelsen, O., Noe-Nygaard, A. & Rasmussen, J. (eds) The deep drilling project 1980-81 in the Faeroe Islands. Annales Societas Scientiarum Færoensis, 1984, 39–70.

Appendix A

Whole-rock chemical composition of lavas and sediments from the Glyvursnes-1 well, Faroe Islands (plus reference basalts)

Sample_ID		GL1-005	GL1-009	GL1-025	GL1-031	GL1-036	GL1-038	GL1-041	GL1-066	GL1-070	GL1-102
Plug No.		G-01	G-02	G-04	G-05	G-06	G-07	G-08	G-10	G-12	G-13
Facies		core	core	core	breccia	core	sediment	sediment	core	crust	core
SiO_2	%	49,05	48,03	49,61	48,10	49,47	51,47	49,82	48,93	48,67	48,96
TiO_2	%	2,40	3,10	3,04	3,16	3,06	1,53	2,55	2,91	2,83	2,76
Al_2O_3	%	15,03	13,49	13,50	13,54	13,04	13,92	13,42	15,51	13,99	14,50
Fe_2O_3	%	4,61	6,52	4,37	10,16	6,87	11,35	10,64	3,73	6,31	3,24
FeO	%	7,69	7,40	9,34	4,55	7,15	1,11	2,24	8,53	6,91	9,30
MnO	%	0,21	0,22	0,22	0,20	0,21	0,16	0,19	0,21	0,21	0,20
MgO	%	5,85	6,18	5,77	5,84	5,57	4,25	6,09	5,26	5,49	5,97
CaO	%	10,89	10,24	10,01	10,26	9,70	8,25	6,25	10,36	10,61	10,58
Na_2O	%	2,52	2,42	2,65	2,56	2,57	1,80	0,99	2,71	2,31	2,56
K_2O	%	0,46	0,19	0,50	0,48	0,80	2,13	1,29	0,28	0,63	0,28
P_2O_5	%	0,22	0,29	0,29	0,32	0,30	0,17	0,18	0,26	0,26	0,25
Volatiles	%	0,75	1,24	0,65	1,10	0,72	3,25	5,86	0,93	1,30	0,76
Sum, majors	%	99,66	99,31	99,94	100,26	99,44	99,40	99,51	99,62	99,51	99,36
V	ppm	344	384	384	413	377	307	183	349	365	354
Cr	ppm	68	131	91	107	82	173	90	70	67	59
Ni	ppm	59	87	74	88	71	81	69	86	64	71
Cu	ppm	223	244	238	285	292	333	188	239	313	260
Zn	ppm	123	142	143	152	141	110	118	129	133	127
Rb	ppm	0	0	0	0	0	0	0	0	0	0
Sr	ppm	255	268	268	262	258	341	122	284	253	258
Y	ppm	27	41	40	48	41	26	24	27	38	24
Zr	ppm	152	198	202	214	207	100	171	174	183	160
Nb	ppm	8	16	12	17	15	1	7	6	12	1
Mo	ppm	0	0	0	0	0	0	0	0	0	0
Sn	ppm	0	0	0	0	0	0	0	0	0	0
Ba	ppm	32	51	70	59	20	51	0	35	27	65
La	ppm	111	115	123	110	126	28	46	78	113	53
Ce	ppm	136	141	143	142	73	79	90	160	139	183
Sum, traces	ppm	1538	1818	1788	1897	1703	1630	1108	1637	1707	1615
Total	%	99,81	99,50	100,11	100,45	99,61	99,57	99,62	99,78	99,68	99,52
Q	Wt%	0,00	1,02	1,30	0,00	1,49	6,36	11,98	1,05	1,37	0,75
Or	Wt%	2,76	1,15	2,98	2,88	4,81	13,23	8,22	1,68	3,81	1,68
Ab	Wt%	21,62	20,98	22,64	22,03	22,14	16,01	9,03	23,29	20,00	22,00
An	Wt%	28,74	26,01	23,67	24,42	22,07	24,81	30,58	29,78	26,54	27,68
Ne	Wt%	0,00	0,00	0,00	0,00	0,00	0,00	0,00	0,00	0,00	0,00
Di	Wt%	20,33	19,94	20,38	20,93	20,69	14,25	1,30	17,13	21,21	19,81
Hy	Wt%	18,91	21,58	19,96	19,46	19,57	19,58	30,77	18,53	18,51	19,79
Ol	Wt%	0,21	0,00	0,00	0,76	0,00	0,00	0,00	0,00	0,00	0,00
Mt	Wt%	2,29	2,60	2,56	2,67	2,60	2,29	2,44	2,31	2,46	2,37
Il	Wt%	4,62	6,03	5,83	6,10	5,92	3,05	5,22	5,61	5,50	5,32
Ap	Wt%	0,52	0,69	0,68	0,75	0,71	0,41	0,45	0,61	0,62	0,59
Sum, norm	Wt%	100,00	100,00	100,00	100,00	100,00	99,99	99,99	99,99	100,02	99,99

'Volatiles' are loss on ignition corrected for oxidation of iron.
Some trace elements are guiding only (compare results on reference basalts). Normative mineral composition is based on a fixed Fe_2O_3/FeO ratio of 0.15.

Appendix A

Whole-rock chemical composition of lavas and sediments from the Glyvursnes-1 well, Faroe Islands (plus reference basalts)

Sample_ID		GL1-143	GL1-179	GL1-213	GL1-214	GL1-217	GL1-224	GL1-225	GL1-229	GL1-239	GL1-265
Plug No.		G-14	G-16	G-17	G-18	G-19	G-20	G-21	G-22	G-23	G-25
Facies		core	core	crust	crust	crust	crust	core	breccia	core	breccia
SiO_2	%	49,05	49,26	48,06	49,54	48,46	48,77	48,61	49,60	48,56	49,55
TiO_2	%	2,70	3,15	3,46	2,39	3,61	3,52	2,82	3,28	3,60	2,86
Al_2O_3	%	14,65	14,89	13,43	16,77	12,15	12,47	14,66	12,29	12,82	14,03
Fe_2O_3	%	4,13	3,64	6,26	5,83	7,33	5,22	8,48	12,74	5,84	10,46
FeO	%	8,62	8,64	7,75	5,17	7,71	9,48	4,63	1,78	9,32	2,65
MnO	%	0,20	0,19	0,21	0,16	0,20	0,27	0,17	0,21	0,23	0,17
MgO	%	5,83	5,78	5,74	4,58	5,17	5,58	5,66	4,88	5,37	5,00
CaO	%	10,72	10,29	10,46	10,40	9,66	9,94	10,06	9,05	9,65	9,64
Na_2O	%	2,58	2,66	2,51	2,73	2,50	2,52	2,60	2,31	2,67	2,41
K_2O	%	0,16	0,41	0,27	0,75	0,50	0,44	0,65	0,75	0,39	0,97
P_2O_5	%	0,24	0,29	0,33	0,21	0,32	0,34	0,25	0,34	0,34	0,24
Volatiles	%	0,91	0,60	1,11	1,22	1,56	0,94	0,76	1,85	0,58	1,10
Sum, majors	%	99,79	99,80	99,59	99,75	99,17	99,50	99,34	99,08	99,36	99,07
V	ppm	370	365	449	317	472	478	351	369	460	359
Cr	ppm	65	190	105	42	103	57	100	24	25	58
Ni	ppm	69	103	65	73	60	61	92	46	55	69
Cu	ppm	228	358	280	171	310	317	269	251	313	264
Zn	ppm	130	129	145	117	152	157	130	143	161	128
Rb	ppm	0	0	0	0	0	0	0	0	0	0
Sr	ppm	271	268	265	294	288	249	265	309	277	277
Y	ppm	31	30	52	16	55	54	32	38	53	26
Zr	ppm	171	191	231	143	240	240	176	209	241	175
Nb	ppm	6	6	18	2	18	17	7	11	18	2
Mo	ppm	0	0	0	0	0	0	0	0	0	0
Sn	ppm	0	0	0	0	0	0	0	0	0	0
Ba	ppm	6	57	117	31	231	6	69	171	69	5
La	ppm	105	61	76	55	127	43	92	44	93	60
Ce	ppm	112	155	172	60	135	164	117	147	193	111
Sum, traces	ppm	1564	1913	1975	1321	2191	1843	1700	1762	1958	1534
Total	%	99,95	99,99	99,78	99,88	99,39	99,68	99,51	99,25	99,56	99,22
Q	Wt%	0,96	1,07	1,07	0,88	2,77	2,03	0,00	5,69	1,48	2,86
Or	Wt%	0,96	2,45	1,63	4,52	3,04	2,65	3,92	4,61	2,34	5,90
Ab	Wt%	22,13	22,74	21,67	23,55	21,79	21,71	22,47	20,33	22,96	21,00
An	Wt%	28,31	27,76	25,07	31,90	21,07	21,80	26,97	21,80	22,20	25,34
Ne	Wt%	0,00	0,00	0,00	0,00	0,00	0,00	0,00	0,00	0,00	0,00
Di	Wt%	19,88	18,06	21,26	16,00	21,79	21,74	18,48	18,83	20,16	18,52
Hy	Wt%	19,61	18,91	19,20	15,99	18,88	19,70	19,63	18,79	20,27	17,83
Ol	Wt%	0,00	0,00	0,00	0,00	0,00	0,00	0,06	0,00	0,00	0,00
Mt	Wt%	2,40	2,30	2,62	2,04	2,82	2,76	2,40	2,64	2,84	2,37
Il	Wt%	5,20	6,02	6,70	4,63	7,06	6,81	5,47	6,48	6,95	5,59
Ap	Wt%	0,56	0,68	0,78	0,50	0,76	0,80	0,59	0,82	0,80	0,57
Sum, norm	Wt%	100,01	99,99	100,00	100,01	99,98	100,00	99,99	99,99	100,00	99,98

'Volatiles' are loss on ignition corrected for oxidation of iron.
Some trace elements are guiding only (compare results on reference basalts). Normative mineral composition is based on a fixed Fe_2O_3/FeO ratio of 0.15.

Appendix A

Whole-rock chemical composition of lavas and sediments from the Glyvursnes-1 well, Faroe Islands (plus reference basalts)

Sample_ID		GL1-280	GL1-294	GL1-297	GL1-302	GL1-306	GL1-340	GL1-345	GL1-346	GL1-352	GL1-354
Plug No.		G-26	G-29	G-30	G-31	G-32	G-33	G-34	G-35	G-36	G-37
Facies		core	core	sediment	crust	crust	core	sediment	crust	core	sediment
SiO_2	%	49,08	48,67	51,82	48,61	48,87	50,05	47,78	43,48	43,94	53,52
TiO_2	%	2,95	2,91	2,77	3,35	3,16	3,23	2,74	0,75	0,66	1,18
Al_2O_3	%	14,51	14,00	13,33	13,30	13,77	13,75	13,39	14,55	14,05	12,56
Fe_2O_3	%	4,53	6,86	8,96	4,17	4,77	4,69	9,80	3,74	2,06	7,15
FeO	%	8,72	6,92	3,25	9,61	8,62	8,44	2,80	5,78	7,84	2,77
MnO	%	0,22	0,21	0,15	0,23	0,22	0,22	0,14	0,19	0,17	0,16
MgO	%	5,64	5,71	5,02	6,04	5,93	5,04	5,57	10,58	13,45	6,45
CaO	%	10,44	10,42	5,42	10,47	10,36	9,90	6,58	9,34	10,29	6,83
Na_2O	%	2,64	2,65	1,08	2,49	2,48	2,63	1,56	1,67	2,00	1,15
K_2O	%	0,19	0,25	4,51	0,17	0,22	0,74	0,72	1,08	0,27	6,05
P_2O_5	%	0,26	0,27	0,17	0,32	0,31	0,34	0,21	0,03	0,02	0,14
Volatiles	%	0,77	0,60	3,61	0,98	0,99	0,60	8,19	8,31	4,72	1,50
Sum, majors	%	99,95	99,47	100,08	99,74	99,71	99,62	99,46	99,49	99,46	99,45
V	ppm	377	383	306	414	392	385	258	191	183	256
Cr	ppm	76	28	62	127	115	51	169	415	461	165
Ni	ppm	74	56	56	68	76	50	86	227	365	68
Cu	ppm	242	235	255	221	238	287	830	119	119	236
Zn	ppm	136	137	121	148	142	141	127	70	74	72
Rb	ppm	0	0	53	0	0	0	0	0	0	2
Sr	ppm	275	275	150	286	285	286	140	72	134	169
Y	ppm	35	40	26	49	43	41	28	0	0	10
Zr	ppm	186	192	189	233	222	228	193	19	13	77
Nb	ppm	11	10	6	18	18	14	6	0	0	0
Mo	ppm	0	0	0	0	0	0	0	0	0	0
Sn	ppm	0	0	0	0	0	0	0	0	0	0
Ba	ppm	52	0	128	0	15	74	56	1043	0	271
La	ppm	163	84	9	63	92	27	115	45	62	0
Ce	ppm	141	93	22	145	126	188	140	125	107	0
Sum, traces	ppm	1768	1533	1383	1772	1764	1772	2148	2326	1518	1326
Total	%	100,12	99,62	100,21	99,92	99,89	99,80	99,68	99,72	99,62	99,58
Q	Wt%	1,16	0,50	5,73	1,58	1,88	2,78	9,89	0,00	0,00	0,00
Or	Wt%	1,14	1,50	27,84	1,02	1,32	4,43	4,70	7,02	1,69	36,72
Ab	Wt%	22,59	22,80	9,55	21,39	21,32	22,54	14,59	15,54	14,45	9,99
An	Wt%	27,48	25,99	19,02	24,98	26,21	23,83	30,30	31,91	30,17	11,54
Ne	Wt%	0,00	0,00	0,00	0,00	0,00	0,00	0,00	0,00	1,85	0,00
Di	Wt%	19,21	20,55	6,51	21,20	19,82	19,66	3,48	15,24	19,02	18,30
Hy	Wt%	19,68	19,86	23,19	20,02	20,11	17,29	28,28	2,91	0,00	16,03
Ol	Wt%	0,00	0,00	0,00	0,00	0,00	0,00	0,00	23,81	29,48	2,96
Mt	Wt%	2,48	2,55	2,26	2,61	2,52	2,45	2,47	1,93	1,96	1,82
Il	Wt%	5,67	5,62	5,50	6,46	6,10	6,21	5,75	1,57	1,32	2,30
Ap	Wt%	0,61	0,64	0,41	0,75	0,73	0,80	0,54	0,08	0,05	0,33
Sum, norm	Wt%	100,02	100,01	100,01	100,01	100,01	99,99	100,00	100,01	99,99	99,99

'Volatiles' are loss on ignition corrected for oxidation of iron.
Some trace elements are guiding only (compare results on reference basalts). Normative mineral composition is based on a fixed Fe_2O_3/FeO ratio of 0.15.

Appendix A

Whole-rock chemical composition of lavas and sediments from the Glyvursnes-1 well, Faroe Islands (plus reference basalts)

Sample_ID		GL1-376	GL1-381	GL1-421	GL1-435	GL1-454	GL1-457	GL1-461	GL1-464	GL1-470	GL1-478
Plug No.		G-39	G-40	G-42	G-45	G-46	G-47	G-48	G-49	G-50	G-52
Facies		crust	core	core	core	crust	core	core	crust	core	core
SiO_2	%	49,86	50,16	47,24	52,29	47,73	48,50	48,35	55,01	48,30	47,93
TiO_2	%	3,12	2,96	3,87	1,27	3,61	2,89	2,86	1,93	2,85	2,75
Al_2O_3	%	13,30	14,29	13,13	11,37	12,36	15,16	14,60	12,00	13,81	14,42
Fe_2O_3	%	6,89	4,14	7,39	2,42	4,77	3,73	4,81	8,30	5,25	3,45
FeO	%	6,42	8,23	7,72	7,82	10,67	9,17	8,42	1,28	7,89	9,01
MnO	%	0,18	0,19	0,22	0,20	0,25	0,20	0,19	0,11	0,19	0,23
MgO	%	5,40	5,06	5,92	11,32	5,99	5,66	5,73	3,69	6,97	6,83
CaO	%	9,44	9,67	10,22	9,55	10,23	10,76	10,61	7,19	10,65	10,77
Na_2O	%	2,52	2,82	2,48	1,91	2,56	2,53	2,37	2,48	2,42	2,25
K_2O	%	0,78	0,33	0,29	0,15	0,37	0,12	0,40	0,83	0,24	0,11
P_2O_5	%	0,30	0,31	0,37	0,11	0,33	0,26	0,25	0,08	0,25	0,24
Volatiles	%	1,39	1,34	0,74	1,39	1,11	0,97	0,76	6,44	0,68	1,30
Sum, majors	%	99,58	99,49	99,58	99,77	99,97	99,94	99,34	99,32	99,49	99,30
V	ppm	334	326	441	239	467	375	364	212	348	346
Cr	ppm	129	113	91	675	102	109	63	153	227	222
Ni	ppm	91	90	80	203	66	75	64	69	114	102
Cu	ppm	308	255	356	90	283	240	192	198	258	224
Zn	ppm	143	136	159	102	163	138	137	82	135	128
Rb	ppm	0	0	0	0	0	0	0	0	0	0
Sr	ppm	274	292	282	210	257	285	274	716	261	258
Y	ppm	37	32	60	0	63	37	37	0	36	29
Zr	ppm	223	214	265	88	249	189	182	113	179	170
Nb	ppm	11	11	23	0	21	10	8	0	9	6
Mo	ppm	0	0	0	0	0	0	0	0	0	0
Sn	ppm	0	0	0	0	0	0	0	0	0	0
Ba	ppm	107	133	57	96	13	13	0	941	0	15
La	ppm	118	101	147	80	122	77	89	11	40	119
Ce	ppm	199	154	180	134	216	152	101	37	153	96
Sum, traces	ppm	1974	1857	2141	1917	2022	1700	1511	2532	1760	1715
Total	%	99,78	99,67	99,80	99,96	100,18	100,11	99,49	99,58	99,67	99,47
Q	Wt%	3,16	3,47	0,16	2,86	0,00	0,73	0,67	16,86	0,00	0,35
Or	Wt%	4,72	1,99	1,74	0,90	2,22	0,72	2,41	5,32	1,44	0,66
Ab	Wt%	21,83	24,37	21,35	16,44	21,97	21,67	20,41	22,77	20,79	19,47
An	Wt%	23,21	25,90	24,25	22,39	21,42	30,02	28,51	20,76	26,52	29,57
Ne	Wt%	0,00	0,00	0,00	0,00	0,00	0,00	0,00	0,00	0,00	0,00
Di	Wt%	18,84	17,44	20,62	20,27	23,17	18,47	19,38	14,38	20,96	19,29
Hy	Wt%	18,98	18,02	20,73	32,47	19,62	19,80	20,04	13,91	20,42	22,38
Ol	Wt%	0,00	0,00	0,00	0,00	0,96	0,00	0,00	0,00	1,32	0,00
Mt	Wt%	2,48	2,34	2,80	1,95	2,91	2,44	2,48	1,82	2,46	2,37
Il	Wt%	6,07	5,74	7,48	2,45	6,95	5,56	5,53	3,98	5,50	5,34
Ap	Wt%	0,71	0,73	0,87	0,26	0,78	0,61	0,59	0,20	0,59	0,57
Sum, norm	Wt%	100,00	100,00	100,00	99,99	100,00	100,02	100,02	100,00	100,00	100,00

'Volatiles' are loss on ignition corrected for oxidation of iron.
Some trace elements are guiding only (compare results on reference basalts). Normative mineral composition is based on a fixed Fe_2O_3/FeO ratio of 0.15.

Appendix A

Whole-rock chemical composition of lavas and sediments from the Glyvursnes-1 well, Faroe Islands (plus reference basalts)

Sample_ID		GL1-483	GL1-493	GL1-502	GL1-508	GL1-514	GL1-545	GL1-546	GL1-551	GL1-570	GL1-588
Plug No.		G-53	G-54	G-56	G-57	G-58	G-60	G-61	G-62	G-64	G-67
Facies		core	core	core	crust	core	core	core	core	core	core
SiO_2	%	48,40	48,54	49,31	50,74	49,53	47,52	48,63	49,86	48,54	48,61
TiO_2	%	3,01	2,86	3,00	2,67	2,10	3,35	2,16	2,35	2,73	2,42
Al_2O_3	%	13,90	15,35	13,89	13,43	16,96	13,73	17,72	16,04	15,98	15,26
Fe_2O_3	%	3,42	4,76	3,49	4,01	2,38	4,10	3,82	3,16	3,18	3,12
FeO	%	9,29	7,47	9,38	7,98	7,52	9,92	6,39	7,57	8,63	8,44
MnO	%	0,22	0,18	0,20	0,19	0,16	0,22	0,14	0,16	0,19	0,18
MgO	%	6,76	5,52	6,18	5,83	5,57	6,25	5,16	5,25	5,06	6,13
CaO	%	10,69	10,54	10,41	10,08	11,16	10,57	10,92	10,84	10,70	11,24
Na_2O	%	2,59	2,59	2,29	2,33	2,43	2,24	2,54	2,64	2,62	2,33
K_2O	%	0,14	0,19	0,19	0,27	0,15	0,13	0,18	0,21	0,18	0,28
P_2O_5	%	0,26	0,25	0,26	0,23	0,18	0,29	0,17	0,21	0,25	0,22
Volatiles	%	1,37	1,11	1,07	1,49	1,14	1,16	1,42	1,07	1,17	1,15
Sum, majors	%	100,05	99,35	99,65	99,25	99,26	99,48	99,25	99,35	99,22	99,39
V	ppm	363	316	355	329	247	386	253	278	311	311
Cr	ppm	255	77	204	153	178	99	88	137	76	191
Ni	ppm	122	84	87	71	84	91	96	81	77	95
Cu	ppm	233	239	244	193	161	282	196	175	228	176
Zn	ppm	135	125	137	130	105	150	106	121	135	123
Rb	ppm	0	0	0	0	0	0	0	0	0	0
Sr	ppm	248	267	265	240	279	263	294	292	292	285
Y	ppm	36	23	37	26	4	45	6	14	26	24
Zr	ppm	189	166	191	169	113	213	115	147	174	156
Nb	ppm	8	3	9	4	0	13	0	0	5	5
Mo	ppm	0	0	0	0	0	0	0	0	0	0
Sn	ppm	0	0	0	0	0	0	0	0	0	0
Ba	ppm	12	24	21	61	0	27	0	1	60	23
La	ppm	70	63	112	49	73	96	55	84	69	99
Ce	ppm	126	128	133	118	82	121	95	99	87	92
Sum, traces	ppm	1797	1515	1795	1543	1326	1786	1304	1429	1540	1580
Total	%	100,23	99,51	99,83	99,40	99,40	99,66	99,38	99,50	99,37	99,54
Q	Wt%	0,00	1,11	2,95	5,53	2,12	0,93	0,92	2,32	1,23	0,51
Or	Wt%	0,84	1,15	1,14	1,64	0,90	0,78	1,09	1,26	1,09	1,69
Ab	Wt%	22,25	22,38	19,69	20,22	20,97	19,32	22,03	22,77	22,65	20,10
An	Wt%	26,28	30,33	27,50	26,04	35,63	27,55	37,32	31,90	31,99	30,95
Ne	Wt%	0,00	0,00	0,00	0,00	0,00	0,00	0,00	0,00	0,00	0,00
Di	Wt%	21,25	17,69	19,20	19,56	16,15	19,83	14,06	17,76	17,01	20,13
Hy	Wt%	19,52	18,91	20,70	19,00	17,83	21,74	18,06	16,90	17,90	19,21
Ol	Wt%	1,04	0,00	0,00	0,00	0,00	0,00	0,00	0,00	0,00	0,00
Mt	Wt%	2,40	2,30	2,43	2,27	1,89	2,66	1,93	2,04	2,25	2,20
Il	Wt%	5,80	5,55	5,77	5,20	4,07	6,49	4,18	4,55	5,30	4,69
Ap	Wt%	0,61	0,59	0,61	0,55	0,43	0,69	0,40	0,50	0,59	0,52
Sum, norm	Wt%	99,99	100,01	99,99	100,01	99,99	99,99	99,99	100,00	100,01	100,00

'Volatiles' are loss on ignition corrected for oxidation of iron.
Some trace elements are guiding only (compare results on reference basalts). Normative mineral composition is based on a fixed Fe_2O_3/FeO ratio of 0.15.

Appendix A

Whole-rock chemical composition of lavas and sediments from the Glyvursnes-1 well, Faroe Islands (plus reference basalts)

Sample_ID		GL1-601	GL1-606	GL1-608	GL1-620	GL1-627	GL1-662	GL1-668	GL1-682	GL1-685	GL1-693
Plug No.		G-70	G-71	G-72	G-73	G-75	G-76	G-77	G-78	G-79	G-80
Facies		core	sediment	core	core	crust	core	core	core	crust	core
SiO_2	%	48,61	50,72	48,56	47,21	45,84	47,68	46,50	46,75	48,42	48,12
TiO_2	%	2,33	2,06	2,46	3,19	3,88	2,96	1,20	1,21	2,51	2,83
Al_2O_3	%	16,38	12,54	15,62	13,83	12,28	15,46	14,78	14,91	14,76	15,20
Fe_2O_3	%	4,20	7,23	3,51	5,49	5,78	5,32	3,02	5,38	5,90	3,96
FeO	%	6,66	3,43	7,78	7,67	8,87	7,06	7,19	5,34	5,40	7,96
MnO	%	0,17	0,20	0,18	0,19	0,22	0,19	0,18	0,18	0,17	0,19
MgO	%	5,47	6,75	5,75	6,31	6,08	5,55	8,41	8,37	5,68	5,78
CaO	%	10,81	5,76	10,98	11,15	10,03	10,06	12,54	12,09	9,55	11,31
Na_2O	%	2,79	0,24	2,58	2,32	2,13	2,97	1,82	1,71	2,73	2,48
K_2O	%	0,14	5,89	0,20	0,12	0,46	0,20	0,08	0,30	0,69	0,11
P_2O_5	%	0,20	0,16	0,22	0,28	0,36	0,27	0,07	0,07	0,24	0,26
Volatiles	%	1,62	4,44	1,64	1,64	3,10	1,57	3,66	3,60	3,32	1,12
Sum, majors	%	99,38	99,41	99,46	99,40	99,02	99,27	99,45	99,92	99,37	99,32
V	ppm	280	226	292	350	415	298	278	273	275	309
Cr	ppm	97	192	139	86	72	76	318	316	91	79
Ni	ppm	63	86	75	90	73	83	147	154	84	67
Cu	ppm	163	358	170	215	263	193	166	160	169	181
Zn	ppm	113	97	116	136	157	126	91	92	115	121
Rb	ppm	0	32	0	0	0	0	0	0	0	0
Sr	ppm	272	176	272	302	260	284	139	98	299	298
Y	ppm	14	21	20	35	57	24	11	15	17	17
Zr	ppm	136	144	140	195	254	177	50	56	154	150
Nb	ppm	0	9	1	13	23	6	0	0	7	0
Mo	ppm	0	0	0	0	0	0	0	0	0	0
Sn	ppm	0	0	0	0	0	0	0	0	0	0
Ba	ppm	0	1079	0	0	6	79	14	0	80	2
La	ppm	35	0	67	60	93	118	56	102	57	59
Ce	ppm	105	0	95	98	215	146	92	118	156	125
Sum, traces	ppm	1278	2420	1387	1580	1888	1610	1362	1384	1504	1408
Total	%	99,51	99,65	99,60	99,56	99,21	99,43	99,59	100,06	99,52	99,47
Q	Wt%	0,00	2,04	0,38	0,05	0,61	0,00	0,00	0,00	0,33	0,48
Or	Wt%	0,85	36,88	1,21	0,73	2,85	1,21	0,49	1,85	4,27	0,66
Ab	Wt%	24,22	2,15	22,36	20,16	18,87	25,82	16,11	15,09	24,16	21,42
An	Wt%	32,58	16,68	31,18	27,69	23,64	29,03	33,38	33,49	27,18	30,64
Ne	Wt%	0,00	0,00	0,00	0,00	0,00	0,00	0,00	0,00	0,00	0,00
Di	Wt%	17,39	10,22	19,07	22,45	21,50	16,88	25,44	23,32	17,08	20,54
Hy	Wt%	17,80	25,48	18,35	19,55	21,12	14,81	11,01	13,65	19,26	17,91
Ol	Wt%	0,09	0,00	0,00	0,00	0,00	3,49	9,03	8,01	0,00	0,00
Mt	Wt%	2,05	2,01	2,15	2,49	2,82	2,34	1,99	2,03	2,15	2,25
Il	Wt%	4,54	4,15	4,78	6,22	7,71	5,78	2,38	2,40	4,99	5,49
Ap	Wt%	0,48	0,39	0,52	0,67	0,87	0,64	0,17	0,17	0,58	0,61
Sum, norm	Wt%	100,00	100,00	100,00	100,01	99,99	100,00	100,00	100,01	100,00	100,00

'Volatiles' are loss on ignition corrected for oxidation of iron.
Some trace elements are guiding only (compare results on reference basalts). Normative mineral composition is based on a fixed Fe_2O_3/FeO ratio of 0.15.

Appendix A

Whole-rock chemical composition of lavas and sediments from the Glyvursnes-1 well, Faroe Islands (plus reference basalts)

Sample_ID Plug No. Facies		In-house reference 871212-1	In-house reference 871212-2	BIR-1 Measured	BIR-1 Recomm.	BR Measured	BR Recomm.	BHVO-2 Measured	BHVO-2 Recomm.	BCR-2 Measured	BCR-2 Recomm.
SiO_2	%	49,70	49,24	47,66	47,80	38,20	38,39	49,92	49,90	54,04	54,10
TiO_2	%	0,77	2,81	0,98	0,96	2,63	2,61	2,73	2,73	2,26	2,26
Al_2O_3	%	17,18	14,18	15,59	15,36	9,99	10,25	13,55	13,50	13,50	13,50
Fe_2O_3	%	3,16	4,91	11,13	11,40	12,67	12,95	12,35	12,30	13,65	13,80
FeO	%	6,29	8,41								
MnO	%	0,17	0,22	0,18	0,17	0,21	0,20	0,18	0,17	0,21	0,20
MgO	%	7,01	5,95	9,62	9,69	13,20	13,35	7,23	7,23	3,59	3,59
CaO	%	13,23	10,56	13,20	13,25	13,57	13,87	11,38	11,40	7,09	7,12
Na_2O	%	1,95	2,57	1,84	1,75	3,07	3,07	2,37	2,22	3,22	3,16
K_2O	%	0,14	0,36	0,01	0,03	1,36	1,41	0,51	0,52	1,78	1,79
P_2O_5	%	0,05	0,25	0,00	0,05	1,15	1,05	0,27	0,27	0,36	0,35
Volatiles	%	0,73	0,47	-0,49		2,78		-0,55		-0,11	
Sum, majors	%	100,37	99,92	99,72		98,82		99,92		99,58	
V	ppm	235	369	300	313	219	236	302	317	384	416
Cr	ppm	171	68	353	382	304	382	244	280	6	18
Ni	ppm	77	77	159	166	271	261	117	119	3	
Cu	ppm	142	232	130	126	75	72	141	127	23	19
Zn	ppm	83	135	86	71	180	161	121	103	148	127
Rb	ppm	0	0	0	0	17	47	0	10	10	48
Sr	ppm	172	270	80	108	1292	1327	380	389	359	346
Y	ppm	4	40	0	16	35	30	23	26	27	37
Zr	ppm	40	184	2	16	258	251	165	172	184	188
Nb	ppm	0	14	0	1	105	98	13	18	6	
Mo	ppm	0	0	0	1	0	2	0	0	0	
Sn	ppm	0	0	0	1	0	3	0	2	0	
Ba	ppm	19	3	25	7	1064	1055	70	130	654	683
La	ppm	91	62	96	1	146	82	97	15	19	25
Ce	ppm	101	135	100	2	183	152	112	38	94	53
Sum, traces	ppm	1135	1589	1331		4149		1785		1917	
Total	%	100,48	100,07	99,85		99,24	0,00	100,10		99,78	
Q	Wt%										
Or	Wt%										
Ab	Wt%										
An	Wt%										
Ne	Wt%										
Di	Wt%										
Hy	Wt%										
Ol	Wt%										
Mt	Wt%										
Il	Wt%										
Ap	Wt%										
Sum, norm	Wt%										

'Volatiles' are loss on ignition corrected for oxidation of iron.
Some trace elements are guiding only (compare results on reference basalts). Normative mineral composition is based on a fixed Fe_2O_3/FeO ratio of 0.15.

Appendix B. Petrography of chemically analysed core samples (see Appendix A)

Sample ID	Top depth (m)	Bottom depth (m)	Associated plug	Lithological unit (from Well Completion Report)	Lithological facies	Petrographic type	PL phen. Vol.%	PL phen max. size (mm)	PL glomerocrysts max. size (mm)
GL1-005	5,64	5,74	G-01	F1	Lava core	Moderately PL-OL-glomerophyric	10	1,4	4
GL1-009	9,78	9,96	G-02	F2	Lava core	Near-aphyric	<1	0,6	0,6
GL1-025	25,99	26,13	G-04	F3	Lava core	Sparsely PL-phyric	2	6	6
GL1-031	31,08	31,20	G-05	F4	Lava breccia	Moderately PL-OL-glomerophyric	15	5	12
GL1-036	36,09	36,28	G-06	F4	Lava core	Sparsely PL-OL-microphyric	2	0,8	0,8
GL1-038	38,93	39,02	G-07	S5	Sediment	Sparsely PL-microphyric	<1	0.2*	-
GL1-041	41,40	41,53	G-08	S5	Sediment	Sparsely PL-microphyric	<1	0.5*	-
GL1-066	66,79	66,95	G-10	F5	Lava core	Highly PL-OL-glomerophyric	30	6	11
GL1-070	70,83	70,99	G-12	F6	Lava crust	Moderately PL-OL-glomerophyric	10	2	5
GL1-102	102,77	102,99	G-13	F6	Lava core	Moderately PL-OL-glomerophyric	7	2,2	5
GL1-143	143,35	143,59	G-14	F6	Lava core	Moderately PL-OL-glomerophyric	15	3	5
GL1-179	179,98	180,17	G-16	F7	Lava core	Highly PL-OL-glomerophyric	25	9	18
GL1-213	213,28	213,37	G-17	F8	Lava crust	Sparsely PL-Ol-glomerophyric	2	2,5	3
GL1-214	214,48	214,60	G-18	F9	Lava crust	Moderately PL-OL-glomerophyric	15	8,5	>12
GL1-217	217,86	217,99	G-19	F10	Lava crust	Near-aphyric	<1	2,3	3
GL1-224	225,89	225,96	G-20	F10	Lava crust	Near-aphyric	<1	>1.5	2,2
GL1-225	225,94	226,13	G-21	F10	Lava core	Highly PL-OL-glomerophyric	20	5,5	>12
GL1-229	229,44	229,51	G-22	F11	Lava breccia	Sparsely PL-Ol-glomerophyric	1	1,7	2
GL1-239	239,26	239,38	G-23	F11	Lava core	Moderately PL-OL-glomerophyric	10	5,5	14
GL1-265	265,82	266,01	G-25	F12	Lava breccia	Moderately PL-glomerophyric	10	6	7
GL1-280	280,37	280,50	G-26	F12	Lava core	Moderately PL-PX-OL-glomerophyric	10	4,3	6,5
GL1-294	294,28	294,38	G-29	F13	Lava core	Moderately PL-OL-glomerophyric	10	2,8	5
GL1-297	297,51	297,62	G-30	S14	Sediment	Sparsely PL-phyric	<1	0,7	-
GL1-302	302,44	302,57	G-31	F14	Lava crust	Near-aphyric	<1	0,6	-
GL1-306	306,63	306,74	G-32	F14	Lava crust	Sparsely PL-phyric	3	4	4
GL1-340	340,74	340,85	G-33	F14	Lava core	Moderately PL-OL-glomerophyric	10	6	6
GL1-345	346,15	346,26	G-34	S15	Sediment	Near-aphyric	<1	0,4	0,7
GL1-346	346,58	346,65	G-35	F15	Lava crust	Near-aphyric	<1	0,5	0,5
GL1-352	353,25	353,38	G-36	F15	Lava core	Near-aphyric	<1	0,9	1,5
GL1-354	355,18	355,25	G-37	S16	Sediment	Sparsely PL-OL-phyric	<1	0,5	-
GL1-376	376,74	376,80	G-39	F16	Lava crust	Sparsely PL-glomerophyric	1	5	5
GL1-381	381,81	381,95	G-40	F16	Lava core	Moderately PL-OL-glomerophyric	10	11	11
GL1-421	421,73	421,82	G-42	F17	Lava core	Sparsely PL-Ol-glomerophyric	2	>6	>6
GL1-435	435,81	435,94	G-45	F18	Lava core	Moderately PX-PL-OL-glomerophyric	3	2,5	2,5
GL1-454	454,66	454,73	G-46	F19	Lava crust	Sparsely PL-PX-microphyric	<1	0.7*	
GL1-457	454,45	454,56	G-47	F19	Lava core	Highly PL-OL-glomerophyric	20	8	10
GL1-461	464,89	464,99	G-48	F20	Lava core	Moderately PL-OL-glomerophyric	10	2,3	7
GL1-464	464,57	464,62	G-49	F21	Lava crust	Near-aphyric	<1	0,5	0,8
GL1-470	464,92	494,97	G-50	F21	Lava core	Near-aphyric	0,1	0,5	0,6
GL1-478	478,86	479,02	G-52	F22	Lava core	Moderately PL-OL-glomerophyric	5	2,8	7
GL1-483	484,21	484,33	G-53	F23	Lava core	Near-aphyric	<1	1,5	-
GL1-493	493,64	493,79	G-54	F24	Lava core	Moderately PL-OL-PX-glomerophyric	15	4,2	7
GL1-502	502,39	502,55	G-56	F25	Lava core	Moderately PL-OL-glomerophyric	10	6,3	8
GL1-508	508,90	509,15	G-57	F26	Lava crust	Moderately PL-OL-glomerophyric	5	2	3,2
GL1-514	514,13	514,36	G-58	F26	Lava core	Moderately PL-OL-PX-glomerophyric	15	6,7	10
GL1-545	545,72	545,91	G-60	F27	Lava core	Moderately PL-OL-glomerophyric	10	10	11
GL1-546	546,46	546,58	G-61	F27	Lava core	Highly PL-OL-PX-glomerophyric	30	8,5	11
GL1-551	551,58	551,75	G-62	F28	Lava core	Highly PL-OL-PX-glomerophyric	20	5,5	7,5
GL1-570	570,71	570,87	G-64	F29	Lava core	Highly PL-OL-glomerophyric	20	3,3	5
GL1-588	589,01	589,16	G-67	F30	Lava core	Moderately PL-OL-PX-glomerophyric	10	3,1	7
GL1-601	602,27	602,41	G-70	F31	Lava core	Mod. PL-OL-glomerophyric	15	2,5	2,5
GL1-606	606,22	606,37	G-71	S32	Sediment	Near-aphyric	<1	0,4	0,6
GL1-608	608,60	608,83	G-72	F32	Lava core	Mod. PL-OL-glomerophyric	15	2,3	3,6
GL1-620	620,24	620,39	G-73	F33	Lava core	Sparsely PL-Ol-glomerophyric	1	2,2	>0.6
GL1-627	627,32	627,40	G-75	F34	Lava crust	Near-aphyric	<1	2,4	2,4
GL1-662	662,87	6,63	G-76	F34	Lava core	Moderately PL-OL-PX-glomerophyric	20	7,8	15
GL1-668	668,67	668,79	G-77	F35	Lava core	Near-aphyric	<1	1,1	-
GL1-682	682,93	683,05	G-78	F35	Lava core	Near-aphyric	<1	0,7	-
GL1-685	685,53	685,94	G-79	F36	Lava crust	Moderately PL-OL-PX-glomerophyric	15	3,5	10
GL1-693	693,79	693,99	G-80	F37	Lava core	Moderately PL-OL-glomerophyric	15	3	7

Note: Microscopic descriptions are based on polished thin sections viewed in tranmitted polarized light at magnification of max. 400 x.

Volume estimates are assisted by the use of a visual comparator.

Petrographic type and phenocryst columns: PL = plagioclase; OL = olivine; PX = pyroxene; phen. = phenocrysts; * = microphemocrysts; max. size of phenocrysts = maximum crystal length.

Groundmass textures: ig = intergranular; h = hyaline; hc = hypocrystalline; is= intersertal; o = ophitic; so = subophitic; mp = microphyric (listed in order of abundance for each sample).

Mesostasis type / Vesicle filling / Clast alteration: c = clay; gl = glass; q = quench; v = void; z = zeolites (listed in approximate order of abundance for each sample).

Vesicle shape / Clast shape: a = angular; irr = irregular; r = rounded; sr = subrounded.

Appendix B. Petrography of chemically analysed core samples (see Appendix A)

Sample ID	OL phen. Vol.%	OL phen. max. size (mm)	OL phen. % alteration	PX phen Vol.%	PX max. size (mm)	Groundmass texture	Mesostasis Vol%	Mesostasis type	Vesicles Vol.%	Vesicles max. size (mm)	Vesicle shape	Vesicle filling
GL1-005	1	1	100	0	0,1	ig	1		3	4	irr	
GL1-009	0	0,3	100	0		ig	5	c	2	8	r-sr	z
GL1-025	0	0,7	100	0,1	0,3	mp	0,5	c	0			
GL1-031	<1	0,7	100	0	0,1	is	abund.	c	10	5	irr-r	v, c
GL1-036	<1	0,4	100	0		ig	<1	c	2	1	irr-r	c
GL1-038	0											
GL1-041	0										r	
GL1-066	1	2	99	<1	0,7	ig-is	5	c	0			
GL1-070	<1	1	100	0		ig	<5	c	10	8	r-irr	c, z
GL1-102	1	1,2	100	0	0,2	ig-(is)	2	c	<1	0,7	r	c
GL1-143	<1	1	100	<1	0,3	ig-is	2	c	0			
GL1-179	2	2,8	100	<1	1	ig	1	c	0			
GL1-213	<1	0,3	100	<1	0,4	ig	5	q, c	10	>10	r-irr	c
GL1-214	1	0,9	100	<1*	0,25	ig-is	10	c, q	15	12	r-irr	c
GL1-217	<1	0,4	100	<1	0,2	ig-is	20	q	20	7	r-irr	c, z, v
GL1-224	0			0		so	5	q, c	10	3	irr-r	c
GL1-225	<1	1,7	100	0		ig-(so)	10	c, q	0			
GL1-229	<1	0,4	100	0		hc			15	7	irr-r	z
GL1-239	1	1	100	0		ig	2	c	0			
GL1-265	0			<1	0,25				10	3	irr-r	z, c
GL1-280	<1	1	100	1	1,2	ig-(is)	3	c	<1	2,5		c
GL1-294	<1	0,7	100	0		ig	2	c	1	1,7	r	c
GL1-297	0			0								
GL1-302	<1	0,5	100	<1	0,3	ig-is	5	q, c	15	7	sr	v
GL1-306	<1	0,4	100	<1	0,3	ig-is	5	q, c	10	3	irr	v, c
GL1-340	<1	0,8	100	0			10	q, c	0			
GL1-345	0			<1	0,2	h						
GL1-346	5	1,2	100	0	0,2	ig	<5	z, c	15	5	r-irr	c, z
GL1-352	10	2	0	0		o	5	z	0			
GL1-354	<1	0,1	100	<1	0,25							
GL1-376	0			0	0,3	ig-is	20	q, c	15	>7	r-irr	v, c
GL1-381	<1	1	100	0	0,3	ig-is	15	c, q	<1	0,8	r-irr	v, c
GL1-421	<1	0,9	100	0	0,2	ig-is	10	q, c	1	1,5	r	c, z, v
GL1-435	1	2	100	10	1,8	is-ig	20	gl, q, c	2	3	r	c
GL1-454	0			<1*	0,4	ig	2	q, c	20	5	irr	v, c
GL1-457	2	1,3	100	<1	0,2	ig	3	q, c	<1	1	r	c
GL1-461	<1	0,7	100	0		ig-(is)	2	q, c	2	5	irr-r	c, z
GL1-464	<1	0,5	100	<1	0,1	ig	<2	q?	50	20	r-irr	z, c
GL1-470	<1	0,3	100	0		ig-(is)	3	c	1	2	r	v, c
GL1-478	<1	0,5	100	<1*	0,5	ig-(so)	2	c	0			
GL1-483	0			0		ig-is	10	c, q	<1	1,5	r	c
GL1-493	<1	0,8	100	<1	0,9	ig-(so)	3	c	<1	0,6	r	c
GL1-502	<1	0,6	100	1*	0,6	ig-is	10	c, q	<1	0,7	r	z?, c
GL1-508	<1	0,7	100	1*	0,3	ig-(is)	5	q	10	5,5	irr-r	z, c
GL1-514	1	1,8	100	<1	0,7	ig-is	5	c	0			
GL1-545	<1	1	100	0		ig-is	5	c	0			
GL1-546	1	2,6	100	<1	0,8	ig-is	15	c, q	5	2,5	irr-r	v, z, c
GL1-551	<1	0,6	100	<1	0,3	ig-(is)	3	c, q	<1	1,3	r	c
GL1-570	<1	0,5	100	<1*	0,4	ig-(is)	3	c	<1	1	r	c, v, z?
GL1-588	1	0,8	100	<1	0,8	ig-(is)	3	c	<1	1,2	r	c, z, v
GL1-601	2	1,5	100	<1	0,2	ig-(is)	3	c	<1	1	r	c
GL1-606	0			<1	0,5							
GL1-608	<1	1,5	100	<1*	0,4	ig-is	5	c, q	1	3	r	c, v
GL1-620	<1	0,9	100	0		ig-(so-is)	5	c, q	5	0,8	irr	v, c
GL1-627	0			0		mp	60	q	15	3,5	irr	c, z, v
GL1-662	2	1,4	100	2	0,7	ig-(is)	3	c	<1	0,4	r	c
GL1-668	1	0,7	5	0		so	3	z, c	0			
GL1-682	0			0		so	10	c, z (1:1)	0			
GL1-685	1	2,6	100	1	1	ig-is	20	q, c	15	7	r-irr	c, z?
GL1-693	1	0,5	100	0		ig-(so)	5	c	0			

Note: Microscopic descriptions are based on polished thin sections viewed in tranmitted polarized light at magnification of max. 400 x.

Volume estimates are assisted by the use of a visual comparator.

Petrographic type and phenocryst columns: PL = plagioclase; OL = olivine; PX = pyroxene; phen. = phenocrysts; * = microphemocrysts; max. size of phenocrysts = maximum crystal length.

Groundmass textures: ig = intergranular; h = hyaline; hc = hypocrystalline; is= intersertal; o = ophitic; so = subophitic; mp = microphyric (listed in order of abundance for each sample).

Mesostasis type / Vesicle filling / Clast alteration: c = clay; gl = glass; q = quench; v = void; z = zeolites (listed in approximate order of abundance for each sample).

Vesicle shape / Clast shape: a = angular; irr = irregular; r = rounded; sr = subrounded.

Appendix B. Petrography of chemically analysed core samples (see Appendix A)

Sample ID	Clast type	Clast min. size (mm)	Clast max. size (mm)	Clast shape	Clast vesicularity	Clast alteration	Comments
GL1-005							
GL1-009							
GL1-025							
GL1-031							
GL1-036							
GL1-038	hyaline	0,02	0,2	shards	low	c	
GL1-041	hyaline	0,02	1,1	scoria	variable	c	Some clasts are subangular
GL1-066							0.2 mm fresh OL in PL
GL1-070							Fine fracture fillings of clay
GL1-102							
GL1-143							
GL1-179							
GL1-213							
GL1-214							
GL1-217							
GL1-224							
GL1-225							
GL1-229		0,2	>23	irr-sr			
GL1-239							
GL1-265							
GL1-280							
GL1-294							
GL1-297	hyaline		0,9	shards	low-high	c, z	
GL1-302							
GL1-306							
GL1-340							
GL1-345	hyaline	0,05	0,9	irr-sr	low-high	c, z	
GL1-346							Olivine difficult to see
GL1-352							Mesostasis partly voids?
GL1-354	hyaline	0,02	0,7	a	low/none	c	
GL1-376							
GL1-381							
GL1-421							
GL1-435							OPX (inclusion-filled)>CPX
GL1-454							
GL1-457							
GL1-461							
GL1-464							Vesicles irregularly distributed
GL1-470							
GL1-478							
GL1-483							
GL1-493							
GL1-502							
GL1-508							
GL1-514							
GL1-545							
GL1-546							
GL1-551							
GL1-570							
GL1-588							
GL1-601							
GL1-606	hyaline	0,05	0,7	irr	high	c	
GL1-608							OL partly elongated
GL1-620							interstitial voids
GL1-627							
GL1-662							
GL1-668							interstitial zeolite-filled voids
GL1-682							interstitial zeolite-filled voids
GL1-685							
GL1-693							interstitial voids?

Note: Microscopic descriptions are based on polished thin sections viewed in tranmitted polarized light at magnification of max. 400 x.

Volume estimates are assisted by the use of a visual comparator.

Petrographic type and phenocryst columns: PL = plagioclase; OL = olivine; PX = pyroxene; phen. = phenocrysts; * = microphemocrysts; max. size of phenocrysts = maximum crystal length

Groundmass textures: ig = intergranular; h = hyaline; hc = hypocrystalline; is= intersertal; o = ophitic; so = subophitic; mp = microphyric (listed in order of abundance for each sample).

Mesostasis type / Vesicle filling / Clast alteration: c = clay; gl = glass; q = quench; v = void; z = zeolites (listed in approximate order of abundance for each sample).

Vesicle shape / Clast shape: a = angular; irr = irregular; r = rounded; sr = subrounded.